

Quantification of active sites in single-site group 4 metal olefin polymerization catalysis

Xavier Desert, Jean-François Carpentier, Evgueni Kirillov

▶ **To cite this version:**

Xavier Desert, Jean-François Carpentier, Evgueni Kirillov. Quantification of active sites in single-site group 4 metal olefin polymerization catalysis. Coordination Chemistry Reviews, 2019, 386, pp.50-68. 10.1016/j.ccr.2019.01.025 . hal-02051155

HAL Id: hal-02051155

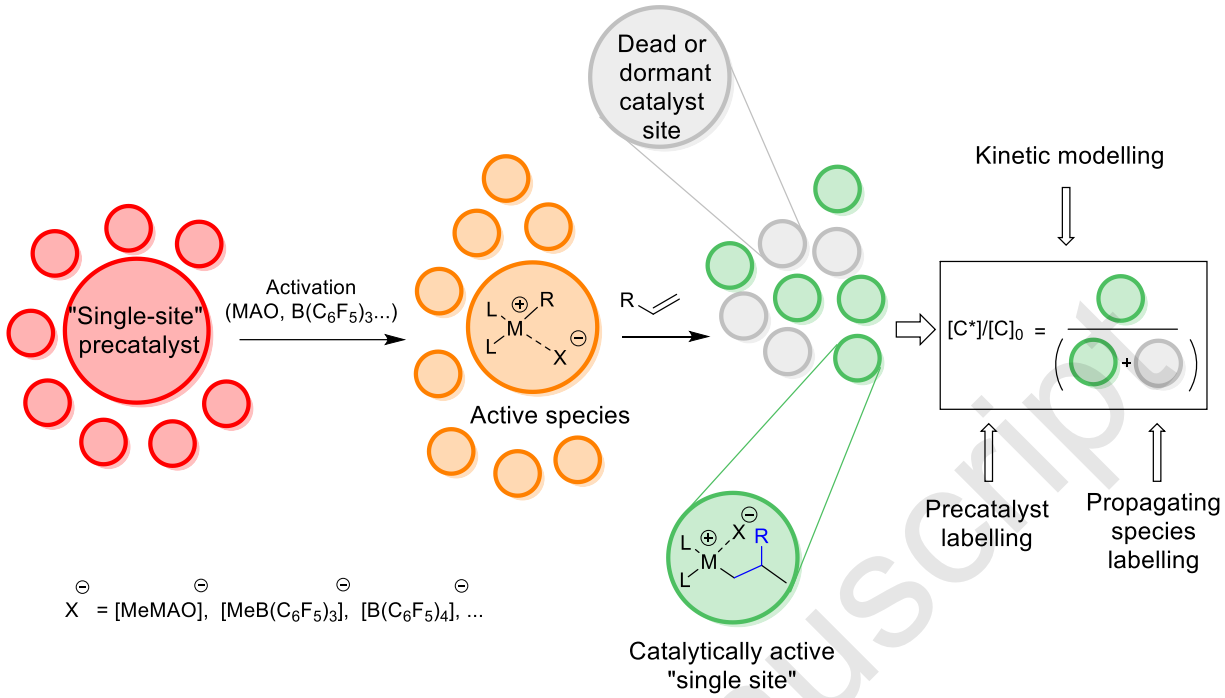
https://univ-rennes.hal.science/hal-02051155

Submitted on 3 Dec 2019

HAL is a multi-disciplinary open access archive for the deposit and dissemination of scientific research documents, whether they are published or not. The documents may come from teaching and research institutions in France or abroad, or from public or private research centers.

L'archive ouverte pluridisciplinaire **HAL**, est destinée au dépôt et à la diffusion de documents scientifiques de niveau recherche, publiés ou non, émanant des établissements d'enseignement et de recherche français ou étrangers, des laboratoires publics ou privés.

For the table of contents



Accepted manuscript

Quantification of Active Sites in Single-Site Group 4 Metal Olefin Polymerization Catalysis

Xavier Desert, Jean-François Carpentier* and Evgueni Kirillov*

Univ Rennes, CNRS, ISCR (Institut des Sciences Chimiques de Rennes), UMR 6226, F-35000 Rennes, France.

Corresponding authors: jean-francois.carpentier@univ-rennes1.fr; evgueni.kirillov@univ-rennes1.fr

Dedicated to Professor Armando J.L. Pombeiro for his outstanding achievements in coordination chemistry and catalysis

Abstract

This review gives an overview of approaches and techniques used for the assessment of active sites count in homogeneous group 4 metal single-site α-olefin polymerization. The main advantages and limitations of these methods, in particular their ability to selectively and quantitatively discern the catalytic sites effectively at work, leaving aside dormant sites and other metal species not directly involved in propagation, as well as the results of their application onto some important single-site olefin polymerization catalyst systems are exemplified. The associated mechanistic information is of interest for engineering more efficient catalytic systems reluctant towards side reactions.

Keywords: α-olefin polymerization; single-site catalysis; group 4 metals; kinetic studies; active sites count

Accepted manuscript

Table of Contents

1. Kinetic modelling 9
1.1. First-principles kinetic modelling 9
1.2. Data acquisition: quench-flow techniques 13
1.3. Modification for batch conditions 15
2. Precatalyst labelling 16
2.1. General considerations 16
2.2. Deuterated tag 18
2.3. UV chromophore tag 18
3. Quench-labelling of metal-polymeryl species 21
3.1. Quench ^{3}H-labelling with MeOT 21
3.2. Quench ^{2}H-labelling with MeOD 22
3.3. Quench-labelling with ^{14}CO 23
3.4. Chromophore quench-labelling 25
3.5. Quench-labelling with O_2 26
3.6. Quench-labelling with Br_2 28
3.7. Quench-labelling with thiophenylcarbonyl chloride (TCC) 29
4. Benchmarking of methods and Molecular catalytic systems 30
4.1. *Ansa*-bis(indenyl) metallocene catalysts and related systems 31
4.2. Unbridged metallocene and half-metallocene catalysts 38
4.3. Post-metallocenes catalysts 41
5. Critical analysis of methods implemented and application studies 48
6. Conclusions 50
7. Acknowledgments 52
8. References 52

Accepted manuscript

Abbreviations

Bn: benzyl

BHT: butyl hydroxylated toluene

C^*: catalytically active site

CGC: constrained geometry catalyst

Chrom: chromophore

Cp: cyclopentadienyl

dMAO: dried methylalumoxane

EBI: 1,2-ethylene-1,1′-bis(indenyl)

EBTHI: 1,2-ethylene-1,1′-bis(tetrahydroindenyl)

FI: phenoxy-imine

Flu: fluorenyl

Ind: indenyl

M: monomer

M_M: monomer molecular weight

M_n: number average molecular weight

M_w: weight average molecular weight

MAO: methylalumoxane

MMAO: modified methylalumoxane

MPS: metal–polymeryl species

MWD: molecular weight distribution

Pol: polymer

P_n: polymerization degree

rac: racemic

SBI: dimethylsilylene-bis(indenyl)

SEC: size exclusion chromatography

TCC: thiophenylcarbonyl chloride

Y: Yield

χ^*: fraction of active sites

Accepted manuscript

Introduction

Single-site catalysis, especially that based on group 4 metals, has brought considerable possibilities in the field of α-olefin polymerization, providing a fine control over the molecular weight and microstructure of the polymers. The high tunability of these molecular catalysts allows for the production of quite different materials, ranging from polyethylene to stereoregular poly(α-olefins) and sophisticated copolymers. As reported in a number of review articles [for a selection, see: 1–10], a considerable diversity of group 4 metal catalyst structures has been designed and synthesized in the past decades. Ubiquitous examples involve the simplest metallocene complexes Cp_2TiCl_2 [11,12] and Cp_2ZrCl_2 [11,13] to the most elaborated ones, such as those derived from {EBI}- [14], {SBI}- [15,16], {Cp/Flu}- [17–20], half-sandwich {CGC}-based [21–24] platforms and more recent post-metallocene systems such as bisphenolate [25,26], Mitsui's phenoxy-imine [27–29] and Dow's pyridyl-amido [30,31] systems (Figure 1), each of them displaying its own behavior and peculiarities in polymerization.

Accepted manuscript

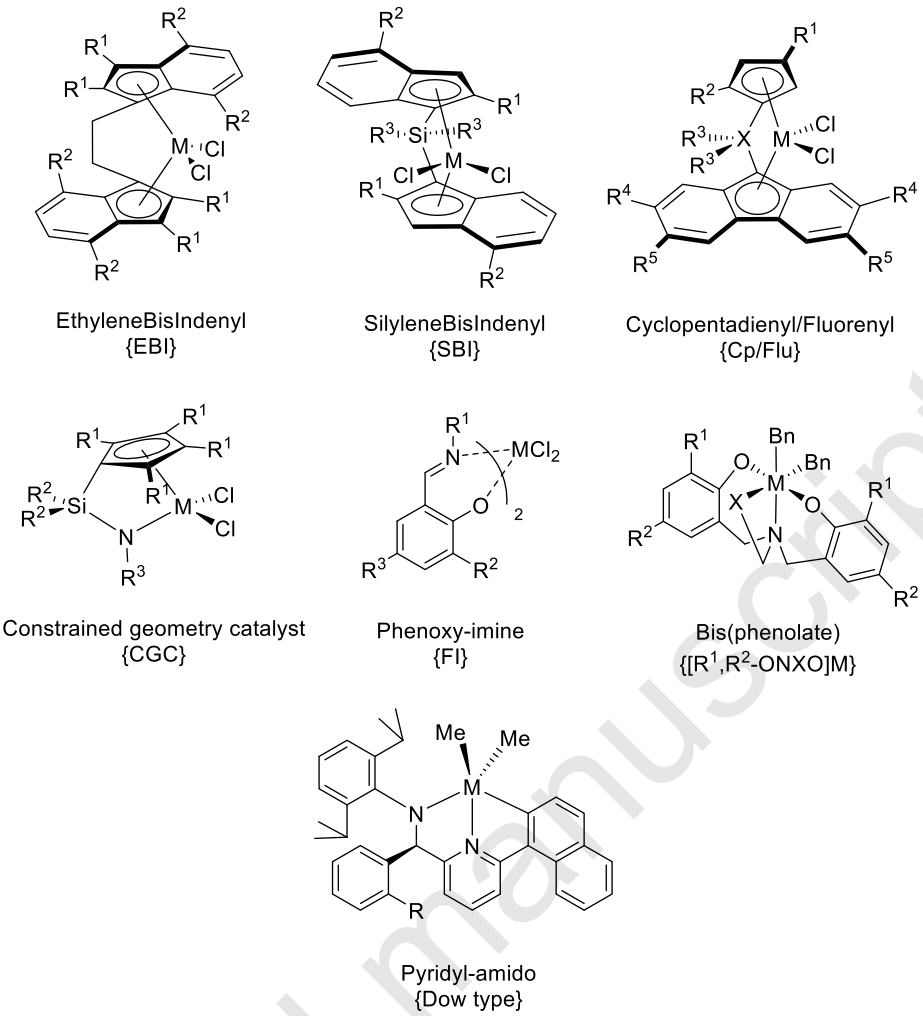


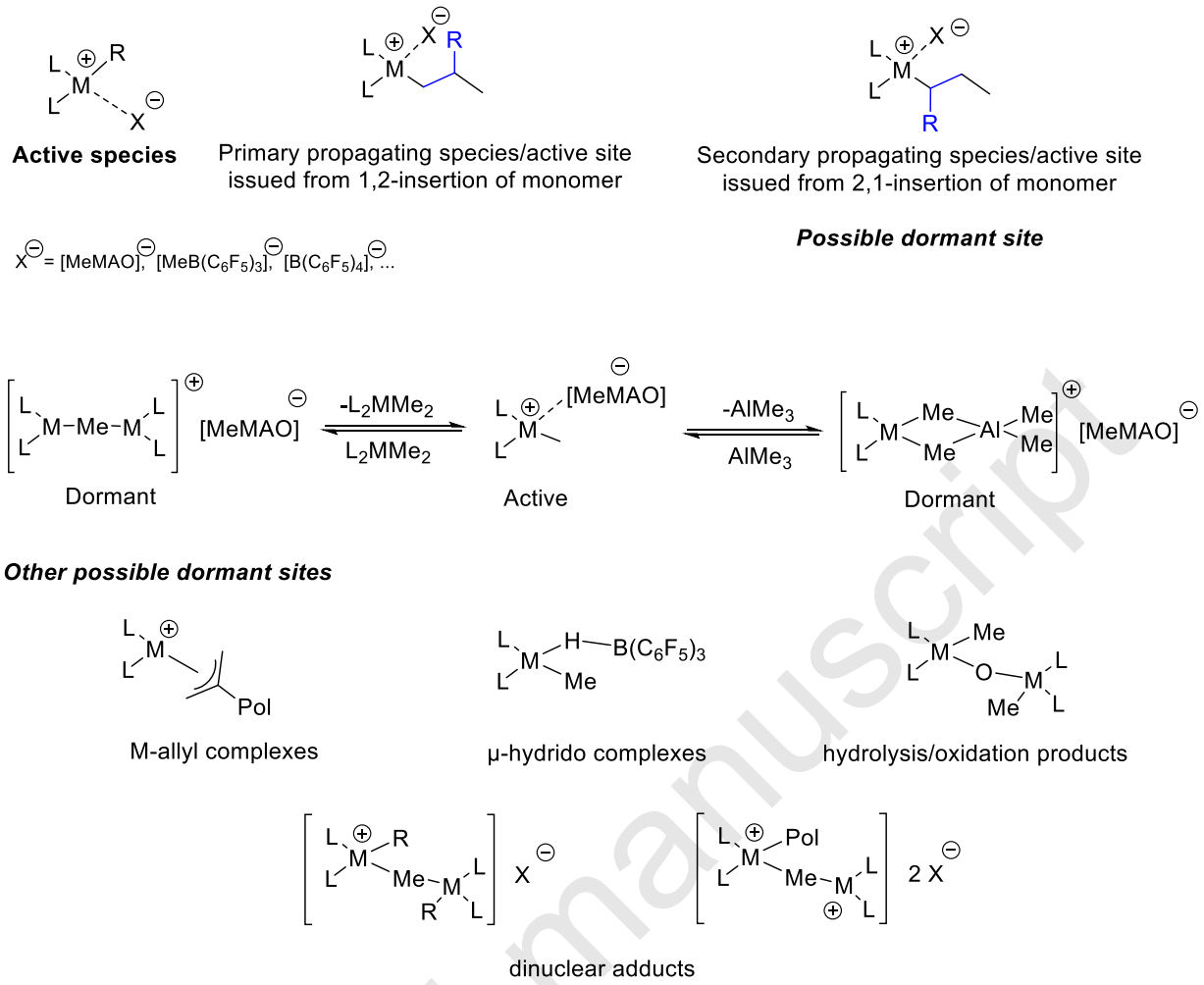
Figure 1. Examples of ubiquitous families of "single-site" group 4 metal precatalysts used for α-olefin polymerization.

Most of the studies conducted on these single-site catalysts usually focused on their productivities and on the properties of the resulting polymers. While these parameters are certainly important to assess industrial relevance, they are not enough to fully apprehend the potential of a catalyst. Maybe surprisingly, studies addressing a deeper understanding of the catalyst behavior through detailed kinetic studies are rather scarce. These investigations were usually aimed at finding kinetic models that can accurately describe the polymerization processes. The related kinetic constants for initiation, propagation, transfer and termination rates can be extracted from a successful fitting of the experimental data to the theoretical model. The

Accepted manuscript

propagation rate quantifies the rate at which an active catalyst site (presumed to be solely or majorly generated from the precatalyst) is able to incorporate monomer molecules in growing polymer chains. Although this value depends on the monomer concentration, temperature and other experimental parameters, it is also essential to remind that it is dependent on the quantity of active catalyst actually involved in chain growth; this one is not necessarily equal, and is actually often significantly lower, to the amount of catalyst precursor introduced. Some studies hypothesize that all (pre)catalyst is active; see e.g. [32–34]. However, even though metallocene, hemi-metallocene and post-metallocene complexes provide *in principle* the same global catalytic environment to all propagating centers (hence the "single-site" nomenclature), it is not guaranteed that they all undergo evenly and entirely the transformation into the active species and that the latter species remain active throughout the polymerization process. In fact, the fragile equilibrium set after the activation step between the catalytically active metal alkyl cation and its counter-ion, issued from the corresponding activator (MAO, $B(C_6F_5)_3$, $[Ph_3C][B(C_6F_5)_4]$…), can be easily perturbed by side-reactions with the precatalyst itself or other organometallic species, impurities, solvent or remaining activator, forming adducts and hetero-bimetallic species that are considered dormant toward polymerization (Scheme 1). In addition, the fraction of catalyst successfully activated can still be deactivated later on, because of other side-reactions (e.g. monomer misinsertions, formation of stable allylic species, etc) during the polymerization, thus altering its overall efficiency.

Accepted manuscript



Scheme 1. Some of the main active and dormant species found in "single-site" group 4 metal-catalyzed α-olefin polymerization (L = Cp-type or equivalent ligand).

Deciphering the exact nature and extent of all these side-species and side-reactions by spectroscopic techniques is often quite complicated, not to say impossible, if one wants to operate under real polymerization conditions. On the other hand, quantifying the number of active sites helps understanding the catalyst behavior during polymerization. Also, having this number of active sites quantified, combined with propagation rate values, offers the possibility of more accurate comparison between catalytic performances of systems, provided that the same conditions and methods were applied to determine these values.

Accepted manuscript

The assessment of active sites count in single-site olefin polymerization requires specific methods and sometimes also specially designed experimental apparatus. This review aims at giving an overview of these techniques, their main advantages and limitations, as well as the results of their application onto some important single-site olefin polymerization catalyst systems. Noteworthy, most of the methods described within this review assess the concentration of active sites [C^*] or their fraction ($\chi^* = [C^*]/[C]_0$) that is set off against the concentration $[C]_0$ of initially introduced precatalyst.

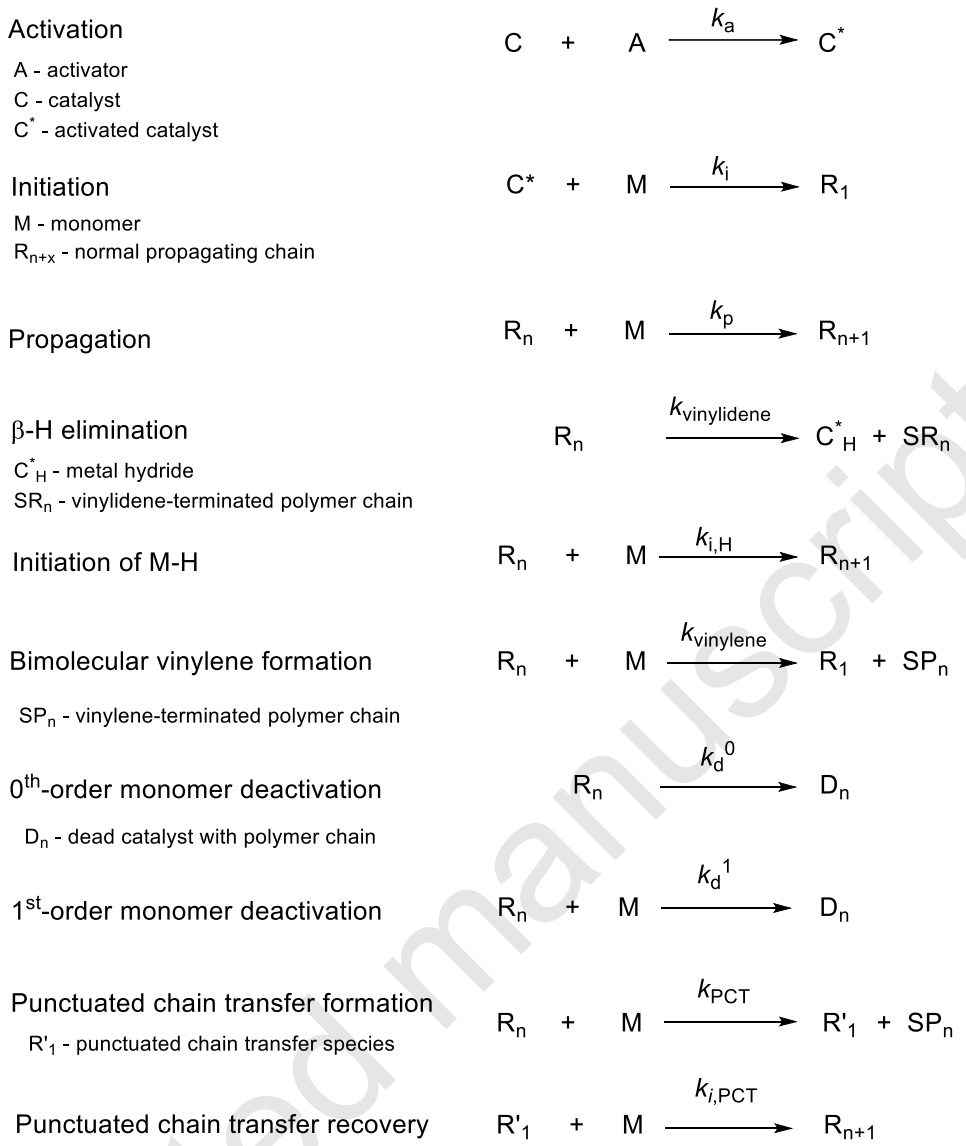
1. Kinetic modelling

Kinetic modelling aims at predicting the behavior of a chemical reaction based on experimental or common knowledge of the system properties. It is by far the most complete method to assess all relevant kinetic parameters of a particular chemical process.

1.1. First-principles kinetic modelling

Numerous efforts have been paid to build a "universal" kinetic model for olefin polymerization processes. A typical approach in these studies is to consider a mechanism with the minimal number of elementary steps that is able to rationalize the experimental data. From these steps, based on first-principles rate law equations, the concentration of species (monomer, active catalyst…) involved in the reaction can be predicted as well as the associated essential kinetic rate constants (k_i, k_p, k_t…). When the model fails to fit the experimental data to a satisfactory extent, additional mechanistic steps must be considered. Typical steps that can be embedded into such a model are chain transfer (to monomer, H_2, AlR_3…), β-H elimination with differentiation between vinyl and vinylidene chain-ends formation, misinsertions (i.e., regioirregular insertions) of the α-olefin monomer, restitution after these misinsertions (i.e., reactivation of a dormant chain), etc. An example of a comprehensive model involving up to 12 elementary processes is delineated in Scheme 2 [35].

Accepted manuscript



Scheme 2. Mechanistic steps for the polymerization of α-olefins by single-site catalysts implemented in the model of Caruthers [35].

The systems of differential equations derived for such comprehensive models usually do not have a straightforward analytical solution and thus, numerical integration methods are widely employed. Therefore, simplified models considering exclusively the propagation and termination steps are more often utilized. In a few cases, for polymerization systems exhibiting induction periods, the initiation step is explicitly embedded into a model as well. Some of the most common simplified models are illustrated below.

Accepted manuscript

A most important but difficult value to determine is the number of active catalyst sites (concentration of propagating species $[C^*]$, or fraction of active sites $\chi^* = [C^*]/[C]_0$). This quantity appears in the rate law of polymerization (1):

$$R_p = -d[M]/dt = k_p[C^*][M]^\alpha \quad (1)$$

where R_p is the polymerization (propagation) rate, k_p is the propagation rate constant, [M] is the monomer concentration and α is the elementary order on monomer.

To simplify the system of equations in their kinetic model, some authors assume arbitrarily an activation efficiency of 100% (i.e., $[C^*] = [C]_0$). This is for instance the case of the study conducted by Estrada and Hamielec for the polymerization of ethylene with the Cp_2ZrCl_2/MAO system [34].

The actual concentration of active species $[C^*]$ (or $[C^*]/[C]_0$) is most usually determined via an independent experimental method (e.g. initial labelling or quench-labelling of propagating species; see Part 2). For this purpose, equation (1) is usually transformed to a simplified representation of the dependence of the polymer yield (Y, in g) as a function of time:

$$Y = k_p[C^*][M]t \quad (2)$$

This model, which assumes $\alpha = 1$ as most often encountered, is valid only in the early stages of the polymerization, at low monomer conversion (<10–20%) when $[M]_t \approx [M]_0$, and where the molecular weight of the polymer increases linearly with time. This regime of "quasi-living" polymerization does not exceed a few seconds in the case of ethylene and propylene whereas it is a matter of minutes, even hours, for higher α-olefins. On the other hand, this situation is most always respected in continuous flow experiments where the monomer is fed continuously into the reactor (see Part 1.4). Also, in this simplified model, the concentration of active sites $[C^*]$ is speculated to remain constant throughout the considered period of time, an assumption which validity is difficult to assess.

In order to determine $[C^*]$, the value of k_p in (2) has to be determined independently via another way. This can be done thanks to a relation of $1/P_n$ as a function of time firstly devised by

Accepted manuscript

Natta [36] for heterogeneous Ziegler-Natta catalysts and later expressed (3) by Busico *et al.* for a homogeneous (e.g. metallocene) catalyst [37]:

$$\frac{1}{P_n} = \frac{M_{\mathrm{M}}}{\overline{M}_{\mathrm{n}}} = \frac{< f_t >}{k_{\mathrm{p}}[\mathrm{M}]} + \frac{1}{k_{\mathrm{p}}[\mathrm{M}]}(1/t) \qquad (3)$$

where P_n is the polymerization degree (acquired through SEC measurements), $<f_t>$ (s^{-1}) is the frequency of chain termination, and k_p ($L \cdot mol^{-1} \cdot s^{-1}$) is the average propagation rate constant (involving both 1,2- and 2,1- insertion modes for α-olefins). It gives an estimation of the k_p value related to the number of metal centers directly involved in growth of polymer chains. As a consequence, the resulting k_p value is associated to *all* catalyst molecules bearing a polymer chain independently of their length or the nature of the active site. The $[C^*]$ value determined in the end is thus the concentration of the metal−polymeryl species at any time during the time scale of the study. Therefore, in this particular case, the method does not discriminate between species resulting from primary (1,2-) and secondary (2,1-) insertion, the latter ones being possible dormant species.

Considering equation (3)**,** the plot of $1/P_n$ vs. $1/t$ must return a linear trace with a slope of $1/k_p[M]$ from which k_p can be extracted. On the other hand, from equation (2), the plot of Y vs. t must give a linear trace passing through the origin with a *slope* = $k_p [C^*][M]_t$. Hence, the value of $[C^*]$ can be retrieved by replacing k_p with its value found from equation (3) and $[M]_t$ by $[M]_0$. The result is often expressed as a fraction of active catalyst, $\chi^* = [C^*]/[C]_0$.

In a situation where an induction period is observed (slower generation of active species, k_i < or ≈ k_p), the initiation step has to be included in the model, which further complicates the equations [37–40]. Bochmann and coworkers applied this methodology to the study of propylene polymerization by *rac*-{Me_2Si(2-Me-4-Ph-1-Ind)$_2$}$ZrCl_2$/MAO and *rac*-{Me_2Si(2-Me-4-Ph-1-Ind)$_2$}$ZrMe_2$/boron activators ($B(C_6F_5)_3$, $[Ph_3C][CN\{B(C_6F_5)_3\}_2]$, $[Ph_3C][B(C_6F_5)_4]$). The equations were modified to include the initiation step in the model, leading to the intricate equation (4):

Accepted manuscript

$$< P_n >$$

$$= \frac{\left(\frac{k_t + k_p[M]_0}{k_t}\right)t + \frac{k_p[M]_0 + k_t - k_i[M]_0}{k_i[M]_0(k_t - k_i[M]_0)}\left(\exp^{-k_i[M]_0 t} - 1\right) - \frac{k_i[M]_0 + k_p[M]_0}{k_t^{2(k_t - k_i[M]_0)}}\left(\exp^{(-k_t t)} - 1\right)}{t + \frac{1}{k_i[M]_0}(\exp^{-k_i[M]_0 t} - 1)} \quad (4)$$

The experimental values of P_n fitted using equation (4) returned the values of k_p and k_t. The model constructed by Bochmann also requires to work at low conversions (or under continuous flow) in order to keep $[M]_0$ constant. This equation was established under the approximation of steady-state conditions (i.e., all catalytic sites released by chain-transfer undergo fast re-initiation without loss). The k_i value was estimated on an average of several kinetic plots; yet, the authors showed that this parameter had minimal influence on the fitting, as changing k_i by two orders of magnitude induced a change of less than 10% in the values of k_p [39]. The fraction of active catalytic sites, $\chi^* = [C^*]/[C]_0$, is finally given by the ratio k_p^0/k_p, where k_p^0 is the apparent propagation rate determined on the whole amount of precatalyst introduced and considering that $[M]_t \approx [M]_0$. Noteworthy again, in these studies, the apparent order in equation (1) is set at $\alpha = 1$, even if the subject is currently open to debate.

1.2. Data acquisition: quench-flow techniques

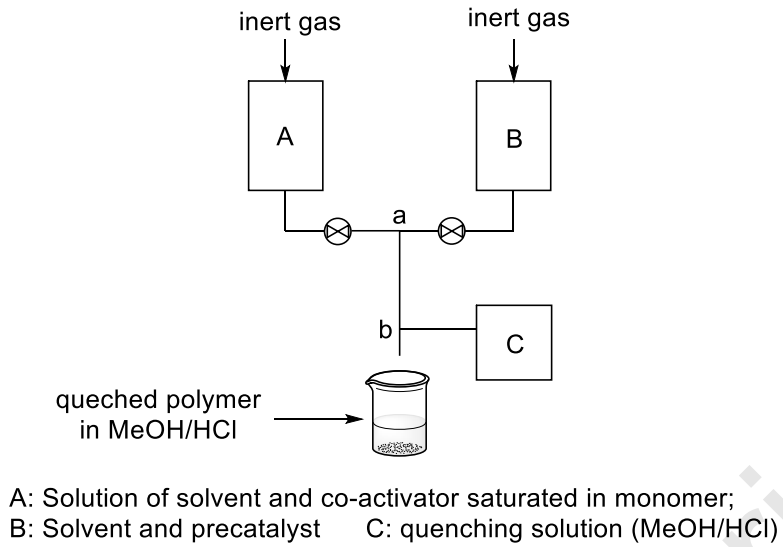
In the early 70s, the Fink [41] and Keii [42] groups introduced a quench-flow technique to study propylene polymerization by traditional heterogeneous Ziegler-Natta catalysts. The approach was later adapted by Busico and coworkers [37] for homogeneous catalysts and used under the name of "stopped-flow" for kinetic studies of ethylene and propylene polymerization with *rac*-{$Me_2Si(2\text{-}Me\text{-}4\text{-}Ph\text{-}1\text{-}Ind)_2$}$ZrCl_2$/MAO [37,43] or {bis(phenoxy-imine)}$TiCl_2$/MAO [43] catalytic systems. Later, Bochmann and coworkers studied by this technique propylene polymerization using *rac*-{$Me_2Si(1\text{-}Ind)_2$}$ZrCl_2$ or *rac*-{$Me_2Si(1\text{-}Ind)_2$}$ZrMe_2$ in combination with MAO or molecular activators, respectively [39,44,45]. An active sites count was also reported by the same group for the post-metallocene CGC system {$Me_2Si(C_5Me_4)N$*t*Bu}$TiCl_2$/

Accepted manuscript

$[Ph_3C][B(C_6F_5)_4]$ [44]. Landis and coworkers also used such technique for studying the polymerization of 1-hexene with the *rac*-{EBI}$ZrCl_2$ system [46].

As mentioned above, the "quasi-living state" condition required by the model approach can be achieved only in the very first stages of the polymerization for ethylene and propylene (ca. 0.1−10 s). This justifies the use of quench-flow techniques that allow measurements of polymer yield and molecular weight on a very short time scale [37,42,47]. The experimental quench-flow setup involves preparation of the different reaction components in separated tanks; these components are mixed under turbulent regime at the entrance (**a**) of the tube-like flow "micro-reactor" and react through their course between points **a** and **b** (Scheme 3). If needed, it is possible to implement several merging points in the apparatus, for example to premix the catalyst and the activator. The monomer and catalyst are thus reacted for a known period of time *t* depending on the dimensions of the tubular "micro-reactor" section (between **a** and **b**) and the flow-rate applied in the apparatus [43]. By adjusting the length and inner diameter of the reactor, very short (0.1−5 s) polymerization times can be gained. The polymerization is then quenched at **b** by a solution of acidified methanol (ethanol) and the polymer is collected. Increases of the polymer yield (Y) and M_n (P_n) of the polymer as a function of time are analyzed to afford rate constants and $[C^*]$.

Accepted manuscript



Scheme 3. Typical setup for quench-flow monitoring studies [37,39,42,43,47,48].

1.3. Modification for batch conditions

The principles of quench-flow techniques have later been adapted for batch [40,46] or semi-batch conditions [34]. Typically, 1-hexene polymerizations proceeded much more slowly than those with ethylene and propylene and can be hence conducted under batch conditions. Thus, Bochmann and coworkers studied the polymerization of 1-hexene with the *rac*-{Me_2Si(2-Me-Benz[e]Ind)$_2$}$ZrCl_2$/MAO system [40]. Consumption of the monomer was monitored by ^1H NMR with respect to an internal standard [46,35,49–57] via analysis of aliquots sampled from the reaction mixture [40].

A peculiar study of a batch propylene polymerization with *rac*-[{Me_2Si(2-Me-Ind)$_2$}$ZrCl_2$ in combination with different co-activators was reported by Naga and coworkers in the late 90s [58]. The polymerization was studied following the principle of quench-flow methods, providing information about polymer yield at different time intervals (assuming no formation of low MW oligomers) and of the corresponding M_n and M_w/M_n values. In order to estimate the fraction of active sites, a different model as compared with Bochmann's and Busico's studies was used, which is expressed as follows:

Accepted manuscript

$$N = \frac{\mathrm{Y}}{\overline{M}_\mathrm{n}} = [\mathrm{C}^*]_t + (k_\mathrm{tr} + k_\mathrm{trA}[\mathrm{Al}] + k_\mathrm{trM}[\mathrm{M}]) \times \frac{\mathrm{Y}}{k_\mathrm{p}[\mathrm{M}]} \quad (5a)$$

$$N = \frac{\mathrm{Y}}{\overline{M}_\mathrm{n}} = [\mathrm{C}^*]_{max} + (k_\mathrm{tr} + k_\mathrm{trA}[\mathrm{Al}] + k_\mathrm{trM}[\mathrm{M}]) \times \frac{\mathrm{Y}}{k_\mathrm{p}[\mathrm{M}]} \quad (5b)$$

where Y is the polymer yield, $[C^*]$ is the concentration of active (propagating) species, k_{tr} the chain-transfer rate constant via β-elimination, k_{trM} the chain-transfer rate constant to monomer, k_{trA} the chain-transfer rate constant to AlR_3, and [Al] concentration of AlR_3 (chain-transfer agent). Parameter *N* as described in (5a) and (5b) links together the average number molecular weight, the polymer yield and the active sites concentration. Its expression differs whether it is used before (5a) the maximum polymerization rate where the maximum amount of active site is not yet reached or after (5b) the maximum polymerization rate where $[C^*]_t = [C^*]_{max}$. Depending on the co-catalyst used, one of the two forms was used. Plotting in both cases N vs. Y returned a linear plot with the intercept at Y = 0 giving the amount $[C^*]_t$ or $[C^*]_{max}$. This method returned a fraction of active catalyst of 8% with MAO and 54% with $AlEt_3/[Ph_3C][B(C_6F_5)_4]$ using (5a). On the other hand, using (5b), only 24% of the initial catalyst concentration with $Al\textit{i}Bu_3/[Ph_3C][B(C_6F_5)_4]$ was found to be active. The authors outlined that these values are a rough estimation (see Part 4).

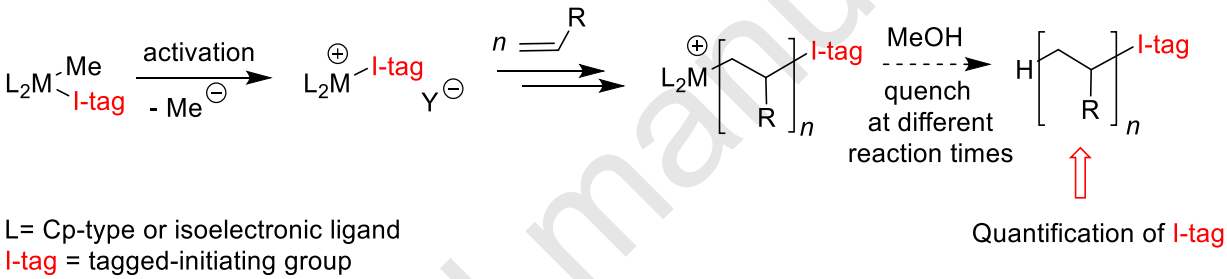
2. Precatalyst labelling

2.1. General considerations

Instead of carrying out tedious kinetic analysis following complex calculations, requiring often many approximations, an alternative way to access the concentration of active sites $[C^*]$ is to implement a chemical label on propagating metal−polymeryl species (MPS). Such label has to be quantifiable by usual analytical techniques. Two main approaches have been reported: tagging the (pre)catalyst to deliver the label onto the growing polymer chain during the initiation step, or directly tagging the active growing MPS with different quenching reagents.

Accepted manuscript

Only a few examples of precatalyst labelling for the quantification of active sites have been reported in the literature. This technique provides an estimate of the number of catalytic centers that were able to participate at least once in the polymerization catalytic cycle (Scheme 4). When the tagged-precatalyst molecule has been successfully activated (with a suitable activator, typically a molecular boron activator) and has undergone the very first insertion step (initiation), the tagged group is transferred onto the terminus of the growing polymeryl chain. This active catalyst propagates and can even initiate new chains upon chain-transfer processes, yet without transferring the label. As a consequence, only the polymer chains resulting from the very first initiation step bear the tag (I-tag, Scheme 4).



Scheme 4. Principle of the evaluation of the initiation efficiency by precatalyst labelling **[**46,49**]**.

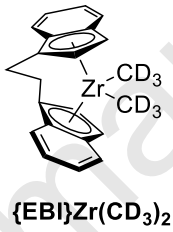
This technique is valid only if the tagged initiating group on the catalyst can be transferred quantitatively onto the polymer and is not lost upon activation, or by irreversible transfer to the co-catalyst or chain-transfer reagents. Consequently, it is not applicable in the presence of chain-transfer activators/agents such as MAO or alkyl-aluminum compounds for example.

This labelling method has been developed by the group of Landis for two different types of tags installed on precatalysts (see Part 4).

Accepted manuscript

2.2. Deuterated tag

The first method of precatalyst labelling consists in the synthesis of a CD_3-tagged zirconocene complex (Figure 2) that is then used as precatalyst for the polymerization of 1-hexene [46,59]. After activation with 1 equiv of $B(C_6F_5)_3$, the polymerization was quenched at regular time intervals and the amount of deuterium in the bulk polymer recovered was then quantified by ^2H NMR (against an internal standard). Such quantification can become tedious, necessitating significant time for correct sample preparation and spectra acquisition. With this approach, Landis and coworkers found that 90% of the labelled catalyst was involved into the initiation step (first insertion) after a period of ca. 70 s.



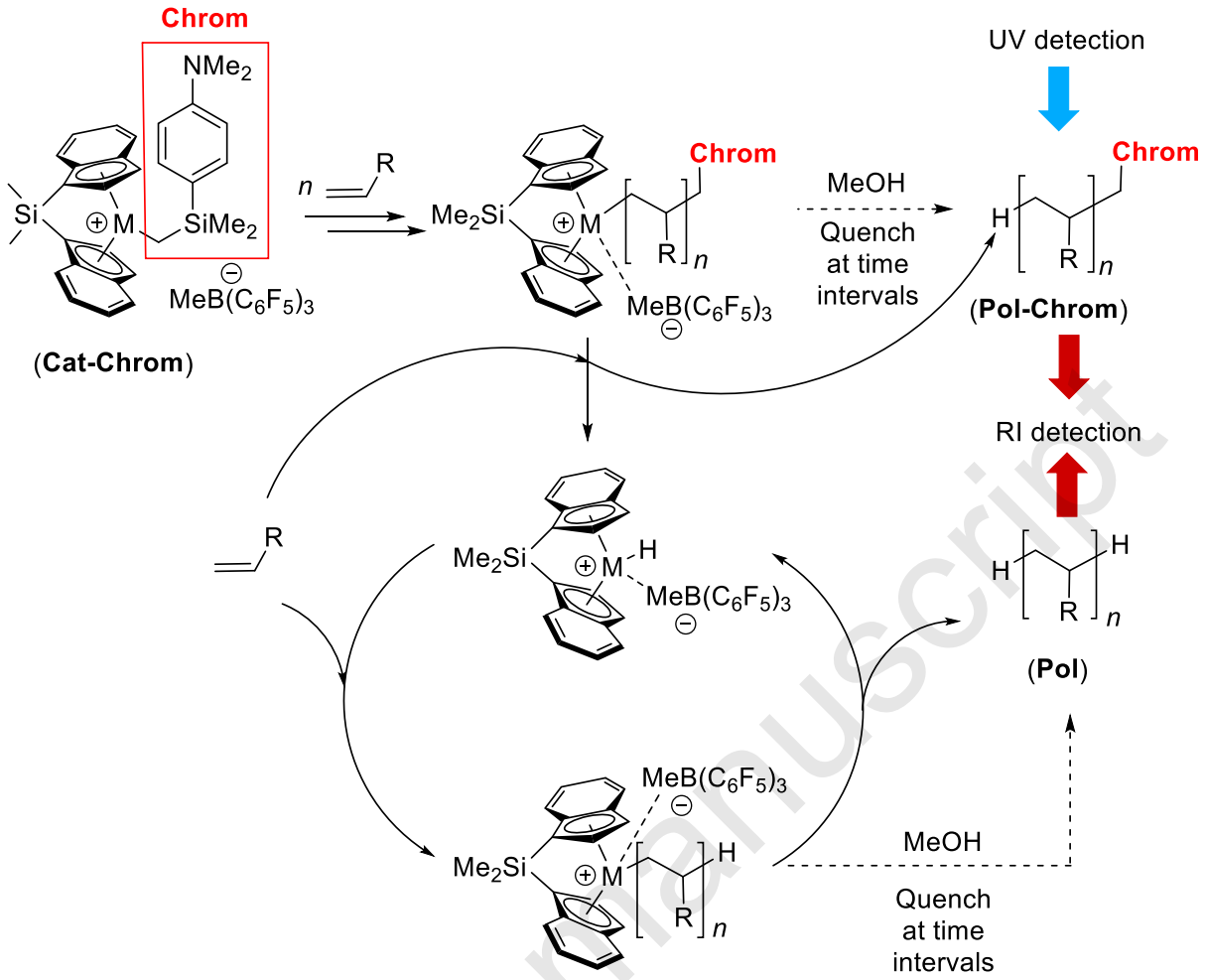
{EBI}Zr(CD$_3$)$_2$

Figure 2. Structure of the modified EBI precatalyst incorporating CD_3 groups as tag **[**46,59**]**.

2.3. UV chromophore tag

The second method involves SEC analysis of chromophore-tagged polymers using UV detection [49]. A chromophore label implemented at the reactive site of the (pre)catalyst (**Cat-Chrom**, Scheme 5) is thus transferred into the first growing polymer chain. The polymers obtained at different quenching times are analyzed by SEC equipped with two detectors: the UV detector provides a trace of mass concentration of the chromophore-bound polymer (**Pol-Chrom**) as a function of the molecular weight, while the second detector, a universal refractive index cell, gives the molar concentration of the bulk polymer chains (i.e., (**Pol-Chrom**) + (**Pol**)) against molecular weight.

Accepted manuscript



Scheme 5. Principle of the UV chromophore-labelling of the catalyst for active sites count [49].

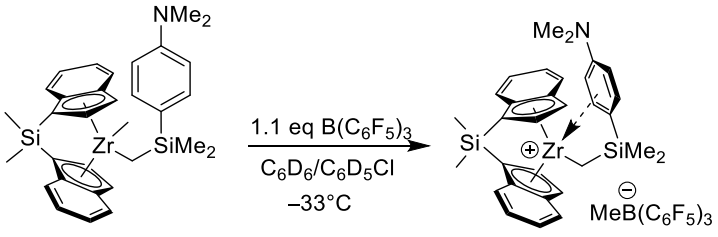
The UV-detection provides significantly enhanced sensitivity as compared to that in the previous study with ^{2}H labelling (vide supra). For example, for a polymer sample prepared at a concentration of 1 mg·mL^{-1}, the method proved competent to detect up to 0.1nM of the **Chrom-cat** species, which corresponds to active site-to-monomer ratios up to 1:10,000 [49]. The sensitivity can be further enhanced by tuning the nature of the chromophore. In comparison, the former ^{2}H labelling study conducted by the same authors was estimated to be only sensitive at best to samples containing more than one active site for 3,000 inserted monomer units [46,59]. This UV chromophore-labelling technique affords different pieces of information about the polymerization process: 1) the molecular weight distribution for the very first chain grown at the

Accepted manuscript

active centers, 2) the molecular weight distribution for bulk polymer, and 3) the fraction of initiated catalyst, i.e. the initiation efficiency.

This UV chromophore-labelling technique was implemented in the study of the industrially relevant catalytic system *rac*-{SBI}ZrMe(Chrom)/$B(C_6F_5)_3$ in 1-hexene polymerization [49]. In order to compare the results provided by the chromophore label with another quantification method, the authors conducted a parallel ^2H labelling/^2H NMR quantification. The polymerization reactions were quenched over the same time intervals with MeOD and the resulting ^2H-labeled polymer chains were analyzed by ^2H NMR spectroscopy. The results obtained by both methods were found to be in perfect accordance, revealing a fraction of initiated catalyst ranging between 12 and 25% of its initial concentration, depending on the conditions used (see Part 4).

One of the limitations of this method discussed by the authors is the possible influence of the chromophore group on the polymerization kinetics. Indeed, the chromophore holds an electron-donating group, possibly leading to the formation of dormant species through interactions with the cationic center of the active catalyst. This fact was evidenced by ^{19}F NMR analysis where the $[MeB(C_5F_6)_3]^-$ anion was found to be displaced from the cationic metal center by the aniline group of the chromophore (Scheme 6). Having a different substituent on the ligand backbone in the close environment to coordination site strongly modifies the initiation rates. On the other hand, as the chromophore group is rejected from the metal center at the terminus of the propagating chain, the propagation rate may remain essentially unaffected.



Scheme 6. Possible deactivation pathway for the chromophore-labelled catalyst [49,50].

Accepted manuscript

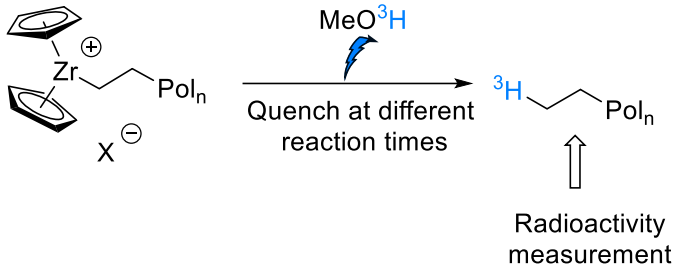
3. Quench-labelling of metal-polymeryl species

3.1. Quench ^{3}H-labelling with MeOT

Radio-labelling techniques using tritiated methanol for active sites count have been pioneered in the mid-80s for traditional heterogeneous Ziegler-Natta type catalysts [60–63]. In early attempts to quantify the number of active species for a metallocene-based system, Chien *et al.* made use of MeO^{3}H (MeOT) to quench the metal−polymeryl species (MPS) in ethylene polymerization with a homogeneous combination of Cp_2ZrCl_2 and a mixture (99:1)[*] of $AlMe_3$ and MAO [64] (Scheme 7). The radioactivity of the polymer recovered was then measured, providing the amount of MPS that was monitored this way over the whole polymerization process by quenching at different reaction times. Yet, since tritiated methanol did not quench selectively only the propagating zirconium centers but also reacted with Al–polymeryl species (eventually resulting from transfer reactions), the amount of MPS thus determined rendered an overestimated count of "active species". On the other hand, extrapolating the evolution of these MPS to the start of the reaction (t = 0) gave an estimation of active centers that have entered the propagation step, i.e. that were initiated at the beginning of the polymerization. A similar MeO^{3}H-quenching/radio-tagging protocol was applied to other catalytic systems such as $CpZrCl_3$/MAO [65], Cp_2ZrCl_2 [65] and (η^5-neomenthyl-Cp)$_2ZrCl_2$/MAO [66]. Typical values for active sites count in these systems ranged from 21% to 95% (see Part 4).

[*] The low amount of MAO used here was justified as a way to reduce the amount of MAO in the polymerization, replacing most of it with $AlMe_3$. MAO was at that time considered dangerous and not worth the risk to use it, considering its low synthetic yield. With this idea in mind, investigating the possibilities to keep a decent polymerization activity while lowering the amount of MAO was of primary interest.

Accepted manuscript



Scheme 7. Principle of polymer chain radio-labelling with MeO^3H [64–69].

Chien and coworkers also investigated propylene polymerization with other catalyst precursors such as *rac*-{EBTHI}ZrX_2 (X = Cl, Me) [67], *rac*-{EBI}ZrX_2 (X = Cl, Me) [68] and *rac*-{1,2-ethylidene(1-$CpMe_4$)(1'-Ind)}TiX_2 [69].

This quenching/radio-tagging method with MeO^3H, despite being quite tedious (calculation of kinetic isotope effect or specific activity of MeO^3H) and hazardous (manipulations of radioactive material), gave the first insights in the quantification of activation for a single-site catalyst. Yet, it has to be reminded that the values were obtained from an extrapolation to t = 0 and the actual evolution of the polymerization between that time and the very first measurement point, is not clearly known; this could tend to over- or underestimate the number of active sites. More problematic, the method is not selective toward MPS and leads to overestimation as the chain-transfer agents are also reactive toward the labelled quenching reactant.

3.2. Quench ^2H-labelling with MeOD

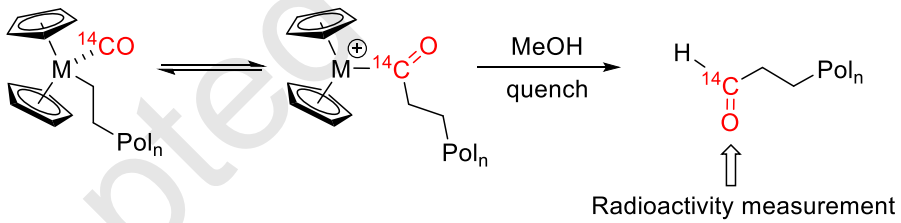
Deuterium quenching is probably the most utilized labelling reagent for active sites count. It was applied by the groups of Landis [46,49,50,59], Abu-Omar [56] and Caruthers [35,51–55,57]. The deuterium label is introduced concomitantly with the quenching reagent; most of the time, MeOD is used, providing both effects at once. The ^2H content in the recovered polymer is quantified by ^2H NMR spectroscopy with respect to an internal standard or using the standard

Accepted manuscript

addition method (vide supra, 2.2.). The amount of ^{2}H found is directly linked to the amount of MPS, including active/propagating catalyst but also possibly to other inactive/dormant species. Hence, this technique also cannot be used with metal-alkyl chain-transfer reagents like $ZnEt_2$ or $AlMe_3$. For that reason, the studies relying on this method often used scavenger-free conditions and activation with a molecular activator.

3.3. Quench-labelling with ^{14}CO

The ^{14}CO radio-tagging method was first applied for heterogeneous Ziegler-Natta catalysts [70–75] and later extended to homogeneous α-olefin polymerization catalyst systems [38,65,76,77]. The method was developed at the same time as the radio-tagging with MeOT discussed above and relies on the insertion of ^{14}C-labelled carbon monoxide into MPS. The polymerization reaction mixtures are allowed to react with an excess of ^{14}CO and the resulting mixture is then subsequently quenched with MeOH (Scheme 8).



Scheme 8. ^{14}CO radio-tagging of polyethylene obtained with the Cp_2ZrCl_2/MAO system **[**64,65**]**.

Despite the ability of ^{14}CO to insert into the Zr−polymeryl species, the method revealed many limitations. One of them is that CO is not a fully effective quenching reagent: while the polymerization is considerably slowed down after CO insertion, further monomer insertions are likely to happen into the M−acyl bond. Also, the CO insertion process was found reversible [72,78,79], which does not guarantee definitive implementation of the label onto the polymer

Accepted manuscript

chain. More, side reactions have been already identified with Ziegler-Natta catalyst systems with this technique [74,77,78,80]. In addition, CO can insert under a fast regime into the Zr–polymeryl bond but can also further react under a slower regime to give multiple insertion products or copolymerization [38,65,76,77]. Hence, in the case of MAO-activated systems, the successive reaction of two molecules of CO with Cp_2ZrMe_2 can lead to an ene-diolate type compound (Figure 3) [65]. It cannot be excluded that a similar side-reaction happens between propagating Zr–polymeryl species and CO. For instance, the group of Busico in an attempt to probe this technique to quantify the number of active sites for the *rac*-[Me_2Si(2-Me-4-Ph-1-Ind)$_2$]$ZrCl_2$/MAO system, unexpectedly ended up at copolymerizing ethylene and CO [77]. Also, the outcome of this method is dependent on the contact time between the propagating species and CO; shorter reaction times (2–4 min) seemed to afford comparable active sites count results with the ^{3}H-labelling (see 3.1.) for the Cp_2ZrCl_2/MAO system [78]. However, for the same catalyst system studied under the same conditions, very different results in active sites count were sometimes reported. Thus, Tait *et al.* claimed that 100% of Zr centers were active in the polymerization of ethylene with the Cp_2ZrCl_2/MAO system [78], but Chien *et al.* found only 10% of catalyst active [65]. For all these reasons, quantification of active propagating centers by ^{14}CO radio-tagging is a difficult method to rely on.

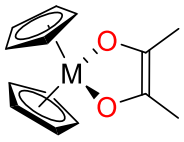
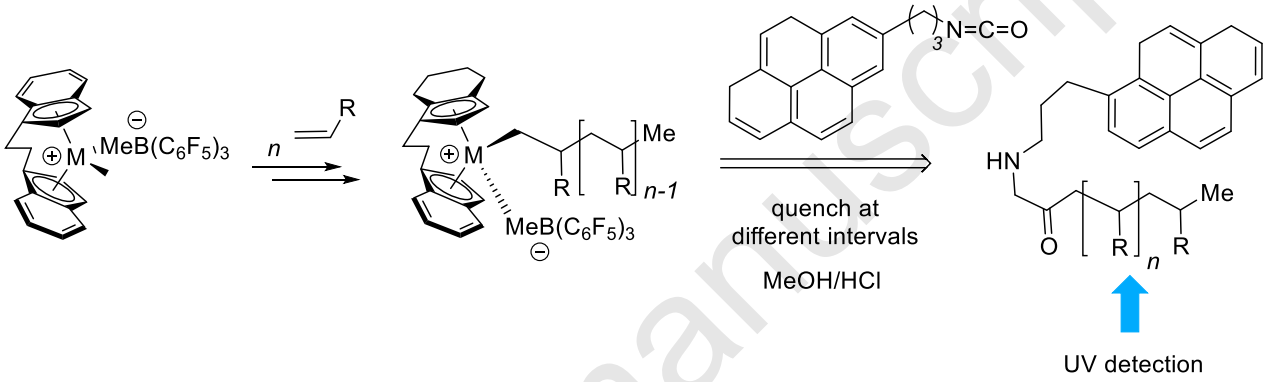


Figure 3. Formation of ene-diolate type compounds upon multiple reaction of Cp_2ZrMe_2 with CO **[**65**]**.

Accepted manuscript

3.4.Chromophore quench-labelling

During the years preceding their initial study on chromophore-labelling of the initiating catalyst sites [49] (see 2.3.) and following the quench-labelling scheme used in the ^2H labelling of metal-polymeryl species, the group of Landis developed new UV-chromophore pyrene derivatives as quenching reagents (Scheme 9) [81]. The number of active sites is recovered through integration of the molecular weight distribution obtained through UV detection at different quenching times.



Scheme 9. Chromophore-labelling of propagating species with an isocyanato-pyrene derivative developed by Landis and co-workers [81].

Three pyrene derivatives were studied as potential candidates for 1-hexene polymerization with the *rac*-{EBI}$ZrMe_2/B(C_6F_5)_3$ system: an isocyanate derivative, an aldehyde analogue and a nitrile-capped one. While with this catalyst system, the latter nitrile reagent revealed no quenching efficiency, both the isocyanate and aldehyde derivatives offered similar capping efficiencies. The fraction of active sites thus determined was found to lie in the range 60–90% of the initially added Zr precatalyst, depending on the conditions used (monomer and catalyst concentrations; see Part 4) [81].

This chromophore quench-labelling method required only a short series of data points (minimum of six experiments) to assess the most important kinetic parameters: active sites count, main rate constants (initiation, propagation, termination, etc.), and molecular weight

Accepted manuscript

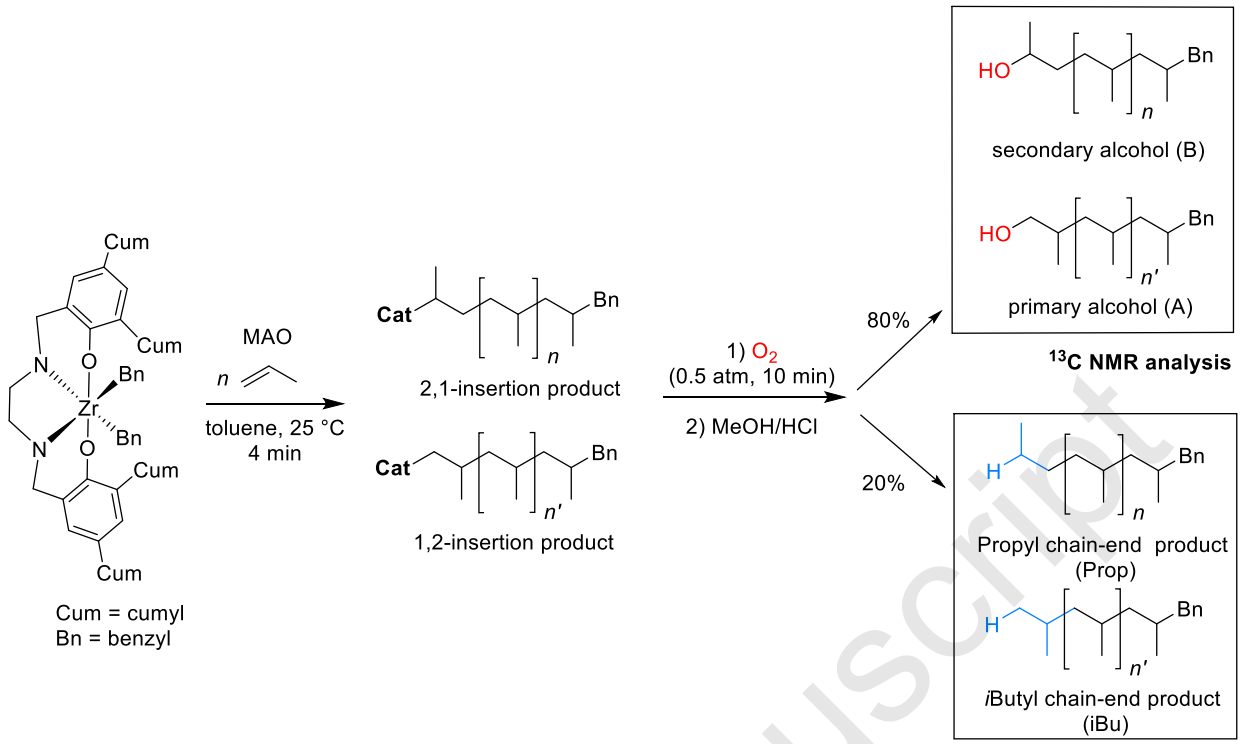
distribution (MWD). This method provides also the "live" evolution of MWD at the different times of quench-labelling.

Most importantly, the method proved selective towards Hf–polymeryl [82–84] species in the presence of $ZnMe_2$ and $ZnEt_2$ as chain-transfer agents upon using the isocyanato-pyrene as the quench reagent [83]. In a similar way, a selective count of Hf–polymeryl species in the presence of trisalkylaluminum compounds was achieved with the nitrile-pyrene as the quench reagent [84] (although it was ineffective with the *rac*-{EBI}$ZrMe_2$/$B(C_6F_5)_3$ system; vide supra). This quench-labelling method was used for studying 1-octene polymerization with a Dow's hafnium pyridine-amidinate catalyst; *it* returned quite variable fractions of active sites in the range 3–70%, depending on the conditions, especially the nature of the activator [82] (see 4.3). Yet, to our knowledge, the method has not been evaluated using MAO as co-activator.

3.5. Quench-labelling with O_2

Cipullo and Busico reported a simple method for quench-labelling of Zr–polymeryl chains with pure O_2 yielding, after an acidic work up, macromolecules capped with single hydroxyl groups [85] (Scheme 10). Yet, the O_2 quench-labelling efficiency was about 80%; the remaining 20% of propagating species are quenched by the acidic work-up, affording saturated chain-ends. This evaluation of the molar fractions of different types of chain-ends (including those resulting from 1,2- and 2,1-propagating species) with respect to total precatalyst was made by comparison between experimental ^{13}C NMR data and simulated spectra.

Accepted manuscript



Scheme 10. The O_2 quench-labelling method used by Busico and co-workers [85].

The fraction of active sites, $\chi^* = [C^*]/[C]_0$, was here determined by the following relation:

$$\chi^* \approx mol\ (chains)/mol(Zr) \qquad (6)$$

where *mol (chains) = mol (primary alcohol A) + mol (secondary alcohol B) + mol (iBu) + mol (terminated "dead" chains)* (Scheme 10). The content of *n*-propyl chain-ends was not considered in the calculation of χ^* as they can result from other processes (vide supra). Another approximation is involvement of the content of terminated "dead" chains (formed by β-H elimination) but this one remains low considering the quasi-living state condition of the study.

The fraction of dormant chains, χ_d (i.e., those resulting from the 2,1- last inserted monomer unit) at the time of the quench was calculated as follows:

$$\chi_d = \chi^* \times \chi(\mathrm{B})/[\chi(\mathrm{A}) + \chi(\mathrm{B})]) \qquad (7)$$

Accepted manuscript

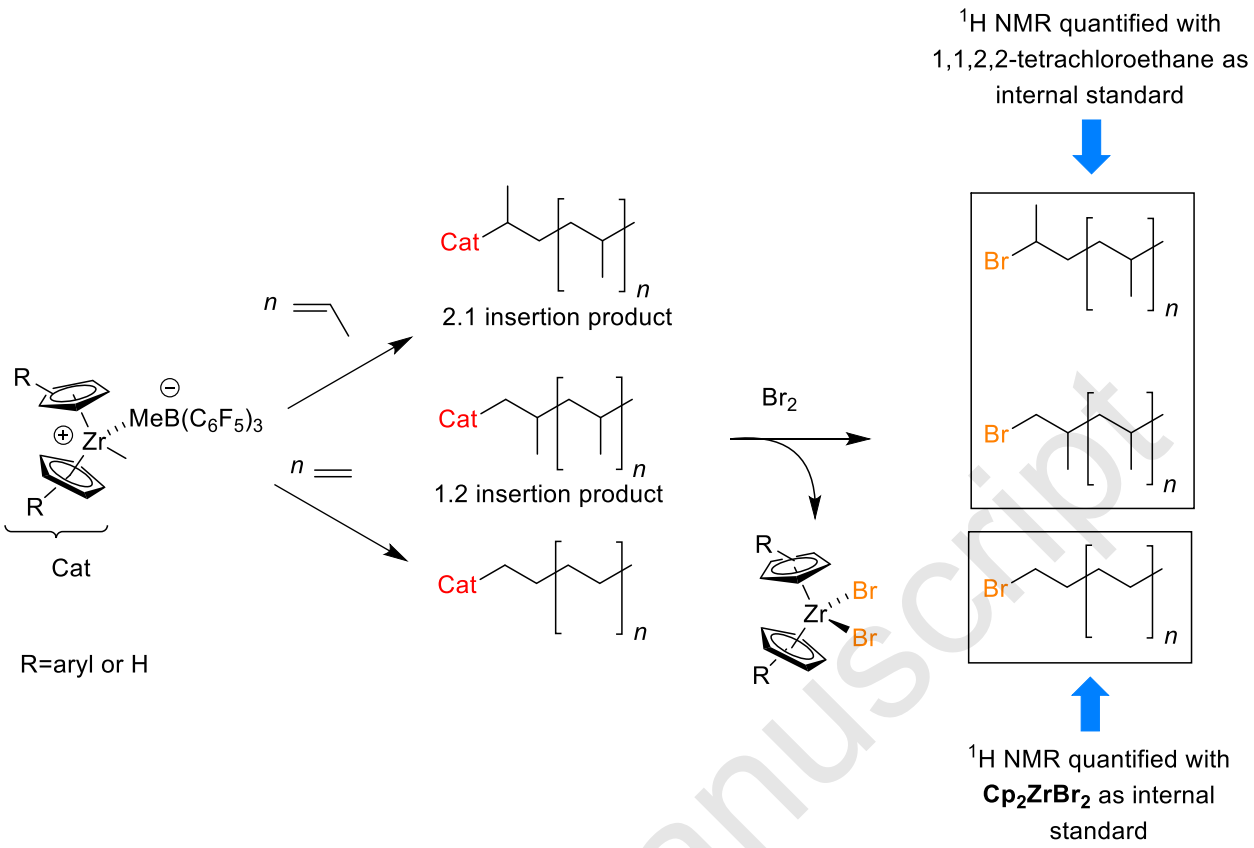
where χ (B) is the fraction of the secondary (2,1-) alcohol chain-ends, χ (A) is the fraction of the primary (1,2-) alcohol chain-ends, and χ^* is the total fraction of active sites (corrected by taking into account the 80% quenching efficiency).

This O_2 quench-labelling technique was applied to the propylene polymerization catalyzed by a Zr{ONNO^{Cum,Cum}}Bn_2/MAO catalyst system (Scheme 10), and returned a fraction of active sites of ca. 40% of the initial precatalyst concentration. The number of polymer chains where the last propylene unit was inserted in a 2,1-fashion accounted for 8% of the total number of active sites. These values are in agreement with those determined using quenched-flow kinetics [86] (see Part 4).

3.6. Quench-labelling with Br_2

A similar process of quench-labelling was developed by Baird and coworkers involving Br_2 as the quenching reagent (Scheme 11) [87]. This technique also allows the differentiation between 2,1- and 1,2- propagating species that are eventually quantified by ^{1}H NMR spectroscopy. This method was probed on the $Cp_2ZrMe_2/B(C_6F_5)_3$ system in ethylene and propylene polymerization and with $(Ind)_2ZrMe_2/B(C_6F_5)_3$ in propylene polymerization. The bromination reaction of the Zr−polymeryl species was quantitative, and allowed an accurate and efficient counting. As quenching with Br_2 also yielded simultaneously the brominated catalyst, which is then trapped in the polymer, the authors used its ^{1}H NMR resonances as an internal standard in the spectroscopic analysis to estimate the amount of propagating species.

Accepted manuscript



Scheme 11. Quench-labelling of propagating species with Br_2 reported by Baird and co-workers [87].

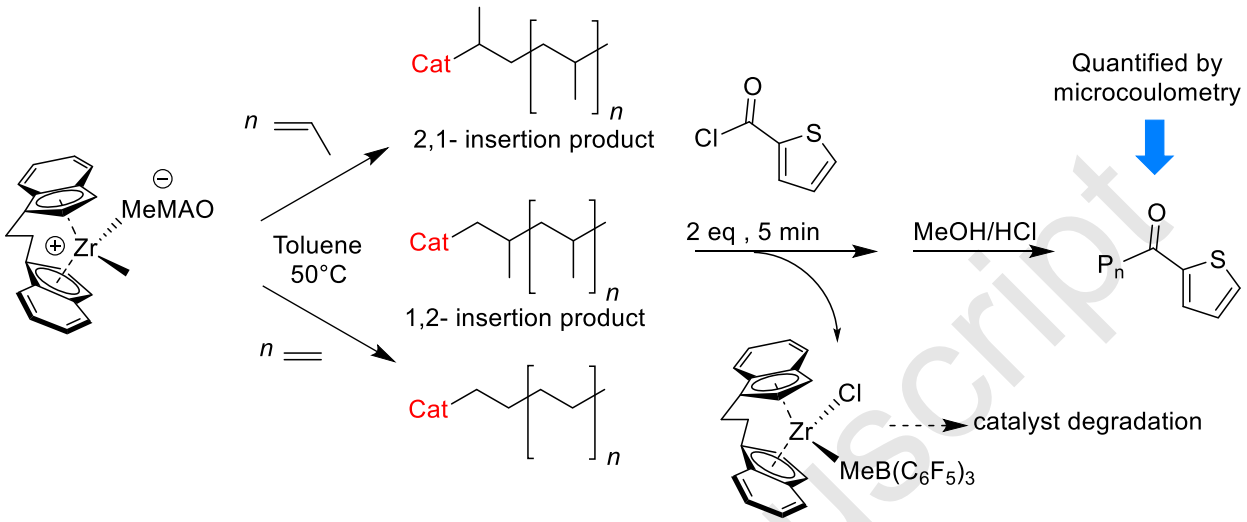
The use of harmful Br_2 as a quenching reagent is one of the method's limitation. Another possible limitation already discussed above is that all propagating species are not trapped by the quenching reagent, yielding underestimated sites counts; this seems unlikely considering the high reactivity of Br_2 but this was not probed independently by the authors.

3.7. Quench-labelling with thiophenylcarbonyl chloride (TCC)

Incorporation into MPS of CS_2 [75] or SO_2 [73] as a labelling reagent was achieved with a limited success. On the other hand, Fan and coworkers developed an effective quench-labelling methodology with heterogeneous Ziegler-Natta catalysts [88–90] that involves thiophenylcarbonyl chloride (TCC). Thus, the polymer chain-ends were capped with sulfur-

Accepted manuscript

containing moieties that were later quantified by microcoulometry (Scheme 12). This method provided a number of informative data on active sites count and propagation rate constants.



Scheme 12. TCC quench-labelling of active species developed by Fan and coworkers for ethylene [91,92] and propylene [92] polymerization with *rac*-{EBI}$ZrCl_2$.

The same authors adapted their methodology to homogeneous single-site catalysts with the ubiquitous *rac*-{EBI}$ZrCl_2$ (Scheme 12) [91,92] to observe the influence of different reaction parameters on the proportion of active sites such as the type of alumoxane coactivator (MAO incorporating different amounts of $AlMe_3$, dried MAO (dMAO), modified MAO containing Al*i*Bu_3 instead of $AlMe_3$ (MMAO)) or the nature of monomer (see Part 4).

4. Benchmarking of methods and Molecular catalytic systems

This section outlines the main results obtained in active sites count with the above described approaches under a wide range of conditions. It specifically aims at emphasizing the relationship between the nature of catalyst systems, both regarding the catalyst precursor and its co-activator, and the resulting fraction of active sites, χ^* (activation efficiency). The results are classified by differentiating several families of homogeneous catalysts that have received special

Accepted manuscript

attention: *ansa*-bis(indenyl)-type metallocenes, unbridged metallocenes and half-metallocenes, and post-metallocenes.

It is important to remind that direct comparison of these data must be conducted with care, because of the intrinsic limitations of the techniques (vide supra and section 5) and also because operating parameters (activation protocol, polymerization conditions) and kinetic/labelling methods have a significant influence on the determined fraction of active sites. This is quite apparent for different catalysts systems, and even so for a given catalytic system probed under variable conditions. Of note, unless otherwise mentioned, all the polymerization results reported hereunder were carried out in toluene.

4.1. *Ansa*-bis(indenyl) metallocene catalysts and related systems

Within the series of *ansa*-bis(indenyl) metallocene precatalysts (Chart 1), the unsubstituted *rac*-{SBI}-zirconocene **1** was studied essentially in propylene and to a lesser extent in 1-hexene polymerization (Table 1, entries 1–5). While activation of the dichloro-metallocene **1a** with MAO (2,600 equiv) resulted only in 8% of active sites at 40 °C [39], slightly better results (13–22%) were obtained upon activation with 1–3 equiv of $[Ph_3C][B(C_6F_5)_4]$ in the presence of Al*i*Bu_3 at room temperature (entries 1 and 2) [44]. Similar fractions of active sites were determined for combinations of the dimethyl-zirconocene **1b** with $[Ph_3C][B(C_6F_5)_4]$ (entry 4). On the other hand, the use of $[Ph_3C][CN\{B(C_6F_5)_3\}_2]$ proved less effective than the two latter boron activators and returned a similar fraction of active sites as with MAO (entry 3).

Accepted manuscript

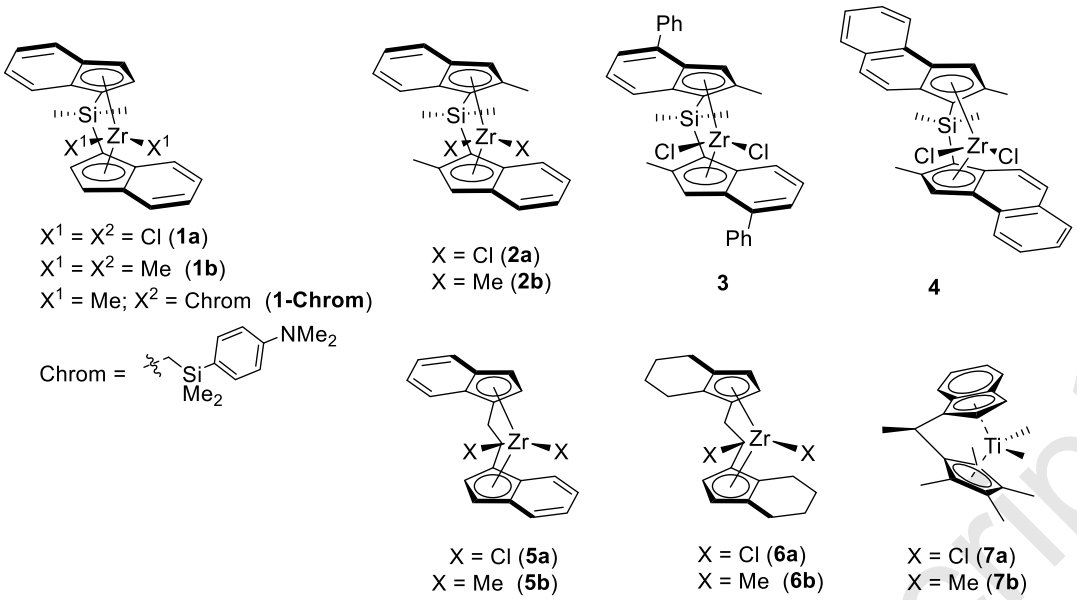


Chart 1. Structures of *ansa*-bis(indenyl)-zirconocenes and related precatalysts investigated in active sites count studies (Table 1).

The series of 2-Me-indenyl substituted zirconocene precatalysts **2** yielded more contrasted results (entries 6−8). The nature of the trisalkylaluminium cocatalyst/scavenger influences significantly the activation efficiency. Thus, the combination of $[Ph_3C][B(C_6F_5)_4]$ with $AlEt_3$ afforded a higher fraction of active sites (χ^* = 54%) as compared to the more "common" combination $[Ph_3C][B(C_6F_5)_4]$/Al*i*Bu_3 that provided only 24% of active sites under otherwise identical reaction conditions [58]. MAO proved less effective (8%, entry 6) but to a similar extent than for **1a** (entry 1).

Busico and co-workers carried out a more extensive study using quench-flow techniques for the bulkier metallocene catalyst **3** in combination with MAO for ethylene and propylene polymerizations (entries 9−12 and 14) [37,43]. Depending on the polymerization temperature and amount of MAO used, from 4% to 23% of active catalyst formed with ethylene. Under similar conditions, Ranieri and coworkers found a fraction of active site of 8% with ethylene at 20 °C [48], thus endorsing the χ^* value of 10% activation found by Busico. Typically, somewhat higher fractions of active species (16−58%) were determined in the polymerization of propylene (entries 14−16).

Accepted manuscript

The influence of different MAO activators was probed by the group of Fan with the *rac*-{EBI} precatalyst **5a** using the TCC quench-labelling technique (entries 19−24). Note that the $[C^*]/[C]_0$ (χ^*) values reported in Table 1 are those determined at 2.5 min; higher fractions of active sites were apparently noted within the same experiment at longer reaction times. However, one must take into account the know ability of TCC to react with $AlEt_3$ at reaction times longer than 10 min [90]. In this regard, it is highly probable here that TCC also quenched $AlEt_3$ and the Al−polymeryl species issued of transfer reactions at higher reaction time. Thus, it is safer to consider the $[C^*]/[C]_0$ values determined at 2.5 min. Changing from regular MAO to dry MAO (dMAO) did not affect significantly the activation efficiency (34% on average); on the other hand, the use of modified MAO (MMAO) induced a slight decrease in the fraction of active sites to 25%. In contrast to the aforementioned Busico's studies on the related Si-bridged catalyst **3**, a significantly lower activation efficiency of this catalyst system was obtained with propylene (8%). Even more striking, Chien and co-workers determined high fractions of active sites for **5a**/$[Ph_3C](B(C_6F_5)_4]$ (χ^*= 94%) and **5a**/$B(C_6F_5)_3$ (χ^*= 77%) for propylene polymerization in combination with $AlEt_3$ at 0 °C (entries 25−26) [68]. A very poor activation efficiency was found for **5b**/$[Ph_3C](B(C_6F_5)_4]$ (χ^*= 2%) and **5b**/$B(C_6F_5)_3$ (χ^*= 4%) but in the absence of $AlEt_3$ (entries 35, 36). The authors came to the conclusion that, in the absence of $AlEt_3$, almost 90% of their precatalyst was lost due to impurities.

Chien and coworkers have investigated the related *rac*-{EBTHI} dichloro-zirconocene (**6a**)/MAO system (entry 37) [67]. At 30 °C, at a low [Al]/[Zr] ratio of 350, a modest activation efficiency was observed (13%). However, when higher [Al]/[Zr] ratios were used (3,500−75,000), the fraction of active sites significantly increased up to 65%. Precatalyst **6b** was also studied for propylene polymerization by the same authors in combination with two different boron activators, $[Ph_3C][B(C_6F_5)_4]$ and $B(C_6F_5)_3$ (entries 38, 39). In both cases, the overall activation efficiency remained very low (2−4%) compared to the **6a**/MAO system.

Accepted manuscript

The more sterically congested titanocene catalysts **7a** and **7b** upon activation with MAO yielded modest activation efficiencies in the range 4−12% in the polymerization of ethylene at − 20 − +20 °C (entries 40, 41).

Several catalyst systems were investigated in 1-hexene polymerization. The combination **4**/MAO afforded a broad range of active sites fractions (13−46%) depending on the $AlMe_3$ content of the MAO used; the more $AlMe_3$, the more active sites produced (entry 17). Combinations of precatalyst **4** pre-activated with MAO and a variety of trisalkylaluminum afforded fractions of active sites that were somehow lower (9−18%, entry 18).

With *rac*-{EBI)$ZrMe_2$ (**5b**), activation protocols involving borane and borate-based compounds provided high fractions of active sites (57−90%), as convincingly demonstrated by different techniques (entries 27−34). Of note, in sharp contrast with $B(C_6F_5)_3$, "activation" of **5b** with $Al(C_6F_5)_3$ resulted in a minimal (1%) efficiency (entry 33). Using the **5b**/$B(C_6F_5)_3$ system, Caruthers reported a relatively lower χ^* value of 57% (entry 27) [35], as compared to the value of 90% obtained by Landis and coworkers on the same system (entries 30, 31) [46]. Despite extensive verifications of their solvents, pre-catalysts and monomer purities, they were not able to explain this discrepancy. Yet, it is noteworthy that the active sites count by Caruthers was conducted at higher conversion (90%) than Landis (8%), which may account for the observed difference.

The Landis group also reported low fractions of active sites (1−21%) for 1-hexene polymerization performed by the combination of pre-catalyst **1-Chrom** with $B(C_6F_5)_3$ (entry 5) [49]. However, the same authors highlighted in a complementary study an interaction between the chromophore group attached to the pre-catalyst and the cationic center of the active species (Scheme 6) [50]. In fact, they estimated that 60% of their catalyst was dormant due to this interaction. This illustrates the possible detrimental effects intrinsic to the method in active sites count.

Accepted manuscript

Concerning 1-hexene polymerization, it must be noted that all high values of fractions of active sites count were conducted at low (0 °C) or very low temperature (–33 °C).

Accepted manuscript

Table 1. Overview of active sites count results obtained for *ansa*-bis(indenyl)zirconocene precatalysts (Chart 1).[a]

Entry	Catalyst (μM)	Monomer (M)[b]	Activator (equiv)	Temp (°C)	Active sites count method	$[C^*]/[C]_0$ (%)	Ref
1	**1a** (146)	P (0.42)	MAO (2,600)	40	Quench-flow	8	[39]
2	**1a** (48)	P (0.60)	$[Ph_3C][B(C_6F_5)_4]$/Al*i*Bu$_3$ (1 or 3:10)	25	"	13 ; 22	[44]
3	**1b** (95)	P (0.59)	$[Ph_3C][CN\{B(C_6F_5)_3\}_2]$/Al*i*Bu$_3$ (1:100)	25	"	8	[39]
4	**1b** (48)	P (0.59)	$[Ph_3C][B(C_6F_5)_4]$/Al*i*Bu$_3$ (1 or 3:10)	25	"	15 ; 16	[44]
5	**1-Chrom** (1,500-6,000)	H (0.8–0.4)	$B(C_6F_5)_3$ (1)	−33	UV catalyst labelling	1.5–21	[49]
6	**2** (nd)	P (0.51)	MAO (nd)	40	Quench-flow	8	[58]
7	**2** (nd)	"	$[Ph_3C][B(C_6F_5)_4]$/AlEt$_3$ (nd)	"	"	54	[58]
8	**2** (nd)	"	$[Ph_3C][B(C_6F_5)_4]$/Al*i*Bu$_3$ (nd)	"	"	24	[58]
9	**3** (30)	E (0.081)	MAO (2,200)	20	Quench-flow	4	[37]
10	**3** (30)	"	MAO (2,200)	20	"	10	[43]
11	**3** (2.8)	E (0.059)	MAO (12,500)	40	"	10	[37]
12	**3** (1.5)	E (0.045)	MAO (23,300)	60	"	23	[37]
13	**3** (2.5)	E (0.16)	MAO (1,000)	25	"	7	[48]
14	**3** (31)	P (0.34)	MAO (3,000)	40	"	58	[37]
15	**3** (3.6)	P (0.8; 0.34)	MAO (14,000)	15 ; 40	"	26 ; 26	[43]
16	**3** (3.6)	P (0.8; 0.34)	MAO/BHT (14,400:4,720)	15 ; 40	"	23 ; 16	[43]
17	**4** (200)	H (1.6)	MAO (1,000) (different TMA grades)	30	"	13-46	[40]
18	**4** (200)	H (1.6)	dMAO + AlR$_3$ (1,000) (R=Me, *i*Bu, *n*Oct)	30	"	9-18[c]	[40]
19	**5a** (10)	E (1 atm)	dMAO (1,000)	50	TCC quench-labelling	32	[91]
20	**5a** (25)	"	dMAO (1,000)	"	"	36	[91]
21	"	"	MAO (1,000)	"	"	33	[91]

Accepted manuscript

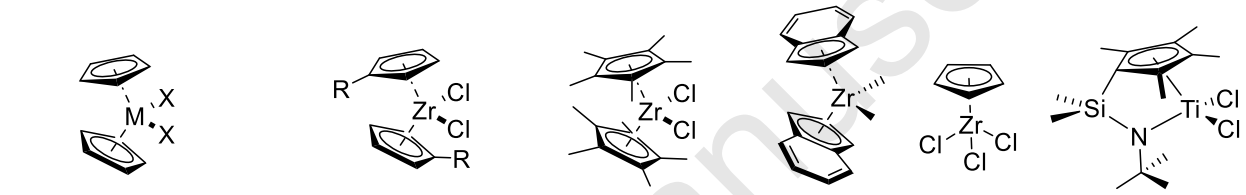
22	“	“	MMAO (1,000)	“	“	25	[91]
23	“	P (1 atm)	“	“	“	8	[92]
24	“	E/P (1atm 1:1)	“	“	“	38	[92]
25	**5a** (10)	P (nd)	$[Ph_3C](B(C_6F_5)_4/AlEt_3$ (nd:125)	0	^{3}H quench-labelling	94	[68]
26	**5a** (25)	P (nd)	$B(C_6F_5)_3/AlEt_3$ (nd:80)	0	“	77	[68]
27	**5b** (2,490)	H (1.0)	$B(C_6F_5)_3$ (1)	0	^{2}H quench-labelling	57	[35]
28	**5b** (2,170)	H (0.5-1.5)	$B(C_6F_5)_3$ (1)	0	UV-Chrom quench-label	84	[81]
29	**5b** (580-2,910)	H (1.0)	$B(C_6F_5)_3$ (1)	0	“	70-84	[81]
30	**5b** (800)	H (1.0)	$B(C_6F_5)_3$ (1)	0	CD_3 catalyst labelling	90	[46]
31	**5b** (800)	H (1.0)	$B(C_6F_5)_3$ (1)	0	^{2}H quench-labelling	90	[46]
32	“	H (1.5)	$B(C_6F_5)_3$ (1)	0	“	90	[59]
33	“	“	$Al(C_6F_5)_3$ (1)	0	“	1	[59]
34	“	“	$[PhNMe_2H][B(C_6F_5)_4]$ (1)	0	“	76	[59]
35	**5b** (350)	P (nd)	$[Ph_3C](B(C_6F_5)_4$ (nd)	0	^{3}H quench-labelling	2.2	[68]
36	**5b** (450)	P (nd)	$B(C_6F_5)_3$ (nd)	0	“	4.4	[68]
37	**6a** (10)	P (0.47)	MAO (350 or 3,500 or 75,000)	30	^{3}H quench-labelling	13-65	[67]
38	**6b** (27)	P (2.2)	$[Ph_3C](B(C_6F_5)_4]$ (1)	30	“	4	[67]
39	**6b** (27)	“	$B(C_6F_5)_3$ (1)	30	“	2	[67]
40	**7a** (27)	E (1.1-2.7)	MAO (2,000)	–20 ; 20	“	3.8-4.5	[69]
41	**7b** (27)	“	“	“	“	4-12	[69]

[a] Polymerizations conducted in toluene; nd: not defined or not determined ; [b] E = ethylene, P = propylene, H = 1-hexene ; concentration in mol·L^{-1}, unless specified in atm; [c] Polymerization conducted in heptane.

Accepted manuscript

4.2. Unbridged metallocene and half-metallocene catalysts

Unbridged metallocene complexes such as **8–11** (Chart 2) with large bite angles feature sterically and electronically quite different coordination spheres as compared to the previous family of *ansa*-bis(indenyl) complexes. This is known to influence significantly their reactivity and may as well affect their activation efficiency. However, establishing clear structure-activation efficiency trends appeared to be tough in that case, due to a limited number of data available and a broad range of reaction conditions used in these studies (Table 2).



M = Zr, $X^1 = X^2$ = Cl (**8a**)
M = Zr, $X^1 = X^2$ = Me (**8b**)
M =Ti, X^1 = Cl, X^2 = Et (**8c**)

R = neomenthyl
9

10 **11** **12** **13**

Chart 2. Structures of unbridged bis(cyclopentadienyl) and related metallocene and half-metallocene precatalysts investigated in active sites count studies (Table 2).

In the polymerization of ethylene, the **8a**/MAO system apparently featured a nearly quantitative activation efficiency at 70 °C (entries 1–3) [34,64,65]. Addition of $AlMe_3$ resulted in a significant drop in active site concentration (entry 4). Strikingly enough, the related molecular system **8b**/$B(C_6F_5)_3$ provided a much lower fraction of active sites, both with ethylene (0.5–5%, entry 5) and with propylene (10%, entries 6–7). The low content of active sites in the latter cases was accounted for by the authors by the possible "encapsulation" of Zr–polymeryl species inside the precipitating polymer during the polymerization course; hence, a significant amount of propagating centers could have escaped the Br_2-quench-labelling process, thus rendering a lower amount of active sites as compared to its real value. Although indeed different

Accepted manuscript

methods were used in these studies, this complete opposition in active sites count points out at major differences between MAO- and molecularly-activated systems.

The more open coordination spheres in half-sandwich complexes **12** and **13** than those typically found in both bridged and unbridged bis(cyclopentadienyl) and related congeners may induce a larger propensity for deactivation of the active species. For the **12**/MAO system (entry 13), the fraction of active sites is apparently highly dependent on the temperature: lowering the temperature from 70 °C to 50 °C induced a drastic drop of the χ^* value from 74% to 21% [65]. Increasing the [Al]/[Zr] ratio from 1,100 to 5,500 did not affect the fraction of active sites (75%); however, at [Al]/[Zr] =10,000, the activation appeared to be nearly quantitative (95%, entry 12).

To our knowledge, **13** is the only CGC complex whose activation efficiency was reported; Bochmann and coworkers studied it under quenched-flow kinetics in propylene polymerization [44]. Though no direct comparison can be made with other catalysts, it is clearly highlighted that for $[Ph_3C][B(C_6F_5)_4]$/[Ti] = 3:1, the fraction of active sites is doubled as compared to a more traditional ratio of 1:1.

Accepted manuscript

Table 2. Overview of active sites count results for unbridged metallocene and half- metallocene catalyst systems (Chart 2).[a]

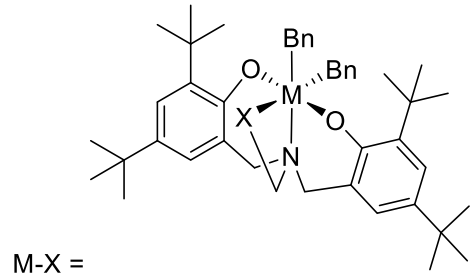
Entry	Catalyst (μM)	Monomer (M)[b]	Activator (equiv)	Temp (°C)	Active sites count method	$[C^*]/[C]_0$ (%)	Ref
1	**8a** (13.1)	E (0.162)	MAO (1,600-3,200)	70	Kinetic modelling	100	[34]
2	**8a** (3.8)	E (1.5 atm)	MAO (10,000)	70	^{3}H quench-labelling	100	[65]
3	**8a** (48)	"	MAO (1,000)	70	"	84	[65]
4	**8a** (51.3)	E (0.118)	$AlMe_3$/MAO (99:1) (1,070)	70	"	40	[64]
5	**8b** (nd)	E (1 atm)	$B(C_6F_5)_3$ (nd)	50	Br_2 quench-labelling	0.5-5	[87]
6[c]	"	"	"	"	"	4-10[c]	[87]
7	"	P (1 atm)	"	"	"	10	[87]
8	**8c** (10,000)	E (0.22)	Et_2AlCl (2 or 4)	10	Quench-flow	5 ; 9	[93]
9	**9** (1.5)	E (0.5 atm)	MAO (30,000)	50	"	51	[66]
10	**10** (2.2)	E (0.1)	MAO (1,000)	25	Quench-flow	14	[48]
11[c]	**11** (nd)	P (1.0 atm)	$B(C_6F_5)_3$ (nd)	21	Br_2 quench-labelling	84[c]	[87]
12	**12** (4)	E (0.162)	MAO (10,000)	70	^{3}H quench-labelling	95	[65]
13	**12** (48)	E (0.162–0.204)	MAO (5,500)	70 ; 50	"	74; 21	[65]
14	**13** (47.5)	P (0.6)	$[Ph_3C][B(C_6F_5)_4]$/Al*i*Bu_3 (1 or 3:10)	25	Quench-flow	15; 34	[44]

[a] Polymerizations conducted in toluene; nd: not defined or not determined. [b] E = ethylene, P = propylene, H = 1-hexene ; concentration in $mol \cdot L^{-1}$, unless specified in atm. [c] Polymerization conducted in chlorobenzene.

Accepted manuscript

4.3. Post-metallocenes catalysts

Among the large number of reported post-metallocene catalysts, only a few structures (Chart 3) were involved in extensive kinetic investigations and active sites count, mostly in the polymerization of 1-hexene (Table 3).

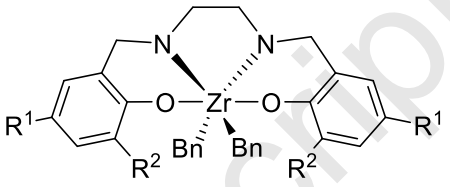


M-X =

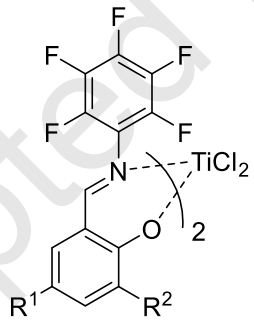
14-Ti Ti-THF
15-Ti Ti-Pyridyl
16-Ti Ti-NMe_2

14-Hf Hf-THF
15-Hf Hf-Pyridyl
16-Hf Hf-NMe_2

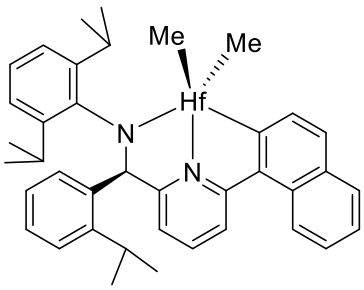
14-Zr Zr-THF
15a-Zr Zr-Pyridyl
15b-Zr Zr-Pyridyl-*p*-CF_3
15c-Zr Zr-Pyridyl-*p*-CH_3
15d-Zr Zr-Pyridyl-*p*-OMe
16-Zr Zr-NMe_2
17-Zr Zr-Furyl
18-Zr Zr-SMe



19 R^1= *t*Bu, R^2 = Et
20 R^1= *t*Bu, R^2 = *i*Pr
21 R^1= *t*Bu, R^2 = *t*Bu
22 R^1= R^2 = Cumyl



R^1= H, R^2 = *t*Bu (**23**)
R^2 = R^1= *t*Bu (**24**)



25

Accepted manuscript

Chart 3. Structures of post-metallocene precatalysts investigated in active sites count studies (Table 3).

A set of studies was reported by Caruthers and coworkers on bis(phenolate)amino-type precatalysts **14–18** upon activation with $B(C_6F_5)_3$ in 1-hexene polymerization (entries 1–18).

Using comparable conditions, the authors probed the influence of several parameters (nature of the metal center [52,55], ligand [53], temperature [57], etc). From this comprehensive work, several conclusions can be drawn concerning the fractions of active sites generated. Noteworthy, these experiments were conducted under scavenger-free conditions that make the active species highly sensitive to impurities.

In general, for all the substitution patterns in this family of zirconium precatalysts, the average fraction of active sites determined at 25 °C was about 50%. The influence of temperature on the active sites count was probed for three substitution patterns in **14-Zr**, **16-Zr** and **18-Zr** (entries 2, 11 and 18). While the temperature did not influence much the behavior of **16-Zr**, the fraction of active sites for **14-Zr** decreased from 83% to 50% along with increase of the temperature (entry 2). The trend for **18-Zr** featured a gradual increase of active sites up to a maximum of 70% at 22 °C and then partial deactivation at higher temperatures (44% at 35 °C) [57].

The influence of electronic factors in the ligand backbone on the production of active sites was probed within a series of differently substituted ligands incorporating a pyridine side-arm bearing electron-withdrawing or -donating groups (entries 5–8). When a simple pyridyl group was used, a χ^* value of 52% was determined (entry 5). Slightly better activation efficiency (58%) was observed for a pyridyl moiety substituted by the electron-withdrawing -CF_3 group. In the same manner, a slightly lower fraction of active sites (47%) was found with the electron-donating -OMe group (entry 8).

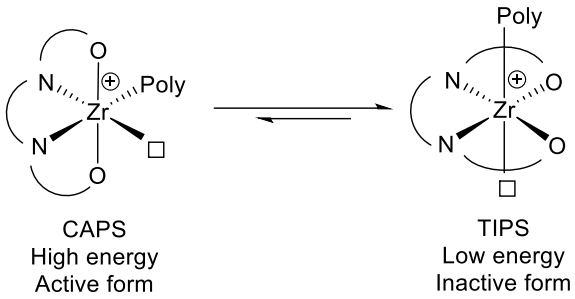
Concerning the nature of the metal center, for an identical substitution pattern on the ligand backbone (same X substituent), the THF-coordinated **14-Ti** and pyridyl-substituted **15-T**i titanium pre-catalysts systematically yielded lower fractions of active sites as compared to their Zr- and Hf-based counterparts (entries 1, 4 vs. 2, 3, 5). This phenomenon was directly linked by the authors to a change of ionic radius between Ti and Zr/Hf; it was proposed that activation could be hindered by the smaller catalytic pocket obtained with the Ti precatalysts. An exception

Accepted manuscript

was observed for the less crowed precatalyst **16-Ti** with X = NMe_2 for which closer activation efficiency, as compared to its Hf and Zr analogues, was observed (entry 10). Within the series of Hf-based catalysts, the different substituents probed had a limited influence on the fraction of active sites; the corresponding χ^* values were found in a narrow 40−50% range. The slightly lower activation for Hf compared to Zr precatalysts was attributed to electronic differences of the metal centers.

Precatalysts **19**, **20** and **21**, similar to precatalyst **16-Zr**, were studied by the group of Abu-Ohmar and Caruthers in 1-hexene polymerization upon activation with $B(C_6F_5)_3$. Both families featured similar fractions of active sites, ranging from 45% to 60% (entries 19−24) as in **16-Z**r (entry 14). Some polymerizations were conducted in bromobenzene (entries 19, 21 and 24) but did not change significantly the fraction of active sites for **20** and **21**; only **19** reached a maximum χ^* value of 83% instead of 60% in toluene. In this series of compounds **19**-**21**, a reversible isomerization process from an active *cis*-form (referred to as CAPS) to an inactive *trans*-form (TIPS) (Scheme 13) was evidenced [94]. In addition to a global active sites count, the authors sought to determine in the fraction of these Zr−polymeryl species the proportion of the active form (CAPS). For all catalysts **19–21**, in toluene, less than 20% of the participating catalyst was converted into the isomerized dormant TIPS form. In bromobenzene, however, the effect was more pronounced, affording 90% and 55% of the inactive TIPS form for **19** and **20**, respectively. The catalytic system **21**/$B(C_6F_5)_3$ appeared to be reluctant to this isomerization with 72% and 99% of active form in toluene and bromobenzene, respectively. This was rationalized by the fact that, when the catalyst undergoes isomerization to the inactive form (TIPS), the *tert*-butyl R^2 substituents face each other. This steric repulsion shifts the equilibrium back toward the active CAPS form.

Accepted manuscript



Scheme 13. Isomerization between the active (CAPS) and dormant form (TIPS) observed for catalysts derived from **17**-**19 [**94**]**.

Compound **22**, which belongs to the same family as **19–21**, was evaluated by two-different methods to be activated at 40% of its initial concentration. The results reported by Busico (entry 26) further indicate that the fraction of active sites in propylene polymerization depends on the operating temperature, with a better activation (χ^* = 39%) at 12 °C than at –6 °C (16%) [86].

Accepted manuscript

Table 3. Overview of active sites count results obtained for post-metallocenes precatalysts (Chart 3).[a]

Entry	Catalyst (μM)	Monomer[b] (M)	Activator (equiv)	Temp (°C)	Active sites Count method	$[C^*]/[C]_0$ (%)	Ref
1	**14-Ti** (900)	H (0.9)	$B(C_6F_5)_3$ (1.1)	25	^{2}H quench-labelling	16	[55]
2	**14-Zr** (300)	H (0.6)	"	–20 ; 0 ; 25	"	83 ; 70 ; 50	[57]
3	**14-Hf** (300)	"	"	25	"	40	[52]
4	**15-Ti** (900)	"	"	"	"	20	[55]
5	**15a-Zr** (300)	"	"	25	"	52	[54]
6	**15b-Zr** (300)	"	"	"	"	58	[54]
7	**15c-Zr** (300)	"	"	"	"	58	[54]
8	**15d-Zr** (300)	"	"	"	"	47	[54]
9	**15-Hf** (300)	"	"	"	"	40	[52]
10	**16-Ti** (900)	"	"	"	"	67	[55]
11	**16-Zr** (300)	"	"	–20 ; 0 ; 25	"	50 ; 50 ; 45	[57]
12	**16-Zr** (500)	H (1.0)	"	"	"	22-45	[51]
13	"	H (0.03)	"	"	"	70	[51]
14	"	H (0.5)	"	"	"	43-67	[51]
15	**16-Zr** (250)	"	"	"	"	39	[51]
16	**16-Hf** (300)	"	"	"	"	50	[52]
17	**17-Zr** (300)	H (0.6)	"	"	"	50	[53]
18	**18-Zr** (300)	"	"	–17 ; 22 ; 35	"	54 ; 70 ; 44	[57]
19	**19** (300)	H (0.09)	"		"	83[c]	[56]

Accepted manuscript

20	**19** (900**)**	“	”	“	“	60	[56]
21	**20** (300)	“	”	“	“	50[c]	[56]
22	**20** (900)	“	”	“	“	60	[56]
23	**21** (900)	“	“	“	“	~45	[56]
24	**21** (900**)**	“	“	“	“	66[c]	[56]
25	**22** (120)	P (1.3)	MAO/BHT (200:270)	25	O_2 quench-labelling	40	[85]
26	**22** (120)	P (2.5, 2.2;1.7)	MAO/BHT (1,300:1,235)	–6 ; 0 ; 12	Quench-Flow	16 ; 28 ; 39	[86]
27	**23** (2.0–10.6)	E (0.5)	MAO (2,000)	60	Quench-flow	24	[48]
28	**24** (4.8)	E (0.07;0.09;0.07)	MAO/BHT (2,800:2,000)	10 ; 25 ; 40	Quench-flow	96 ; 75 ;78	[86]
29	**25** (83)	O (0.5)	$[HNMe(C_{18}H_{37})_2][B(C_6F_5)_4]$ (1.1)	60	UV-Chrom quench-label	3	[82]
30	**“**	“	$B(C_6F_5)_3$ (1.1)	“	“	29	[82]
31	“	“	$[Ph_3C][B(C_6F_5)_4]$ (1.1)	“	“	20	[82]
32	“	“	$[Ph_3C][B(C_6F_5)_4]$ (1.1)	“	“	50-60	[82]
33	“	“	$[Ph_3C][B(C_6F_5)_4]/ZnMe_2$ (1.1:20)	50	“	50	[83]
34	“	“	$[Ph_3C][B(C_6F_5)_4]/ZnEt_2$ (1.1:20)	50	“	50	[83]
35	“	“	$[Ph_3C][B(C_6F_5)_4]/AlEt_3$ (1.1:20)	50	“	16 or 40[d]	[84]
36	“	“	$[Ph_3C][B(C_6F_5)_4]/AlMe_3$ (1.1:20)	“	“	5 or 30[d]	[84]

[a] Polymerizations conducted in toluene. [b] E = ethylene, P = propylene, H = 1-hexene, O = 1-octene. [c] Polymerization conducted in bromobenzene; [d] Different introduction protocols of AlR_3 were used; see text.

Accepted manuscript

The kinetic behavior of phenoxy-imino systems derived from precatalysts **23** and **24** in combination with MAO was investigated in ethylene polymerization by quench-flow kinetics. The **24**/MAO system provided a high fraction of active sites (χ^* = 96%) at relatively low temperature (10 °C) but raising the temperature to 25−40 °C induced a drop in χ^* to ca. 75% (entry 28). Though compound **23** is closely related to **24**, it exhibited only 24% of activation efficiency at 60 °C as determined by the same count methods and under similar conditions (entry 27).

Dow's catalytic system incorporating the pyridine-amido hafnium precursor **25** in combination with different molecular activators was recently studied in 1-octene polymerization by Landis and co-workers using the UV chromophore quench-labelling technique (entries 29−36) [82−84]. While activation with the Brønsted acid $[HNMe(C_{18}H_{37})_2][B(C_6F_5)_4]$ appeared to be ineffective for the generation of active sites (entry 29), activation with $B(C_6F_5)_3$ provided 45% of active sites after an induction period of ca. 45 s. $[Ph_3C][B(C_6F_5)_4]$ afforded only 20% of active sites when used without pre-activation step (entry 31). However, if the precatalyst is pre-activated with $[Ph_3C][B(C_6F_5)_4]$ prior to addition of the monomer, a ca. 50−60% fraction of active sites was obtained without any induction period. This activator and activation protocol was used in subsequent studies aimed at investigating the influence of a chain-transfer agent (entries 33−36). The addition of $ZnMe_2$ or $ZnEt_2$, even at different temperatures for the latter one, did not have any significant influence on the fraction of active sites. On the other hand, with $AlEt_3$ or $AlMe_3$, the fraction of active sites was affected by the polymerizations conditions. When $AlEt_3$ was introduced in the reaction medium from the very beginning, the polymerization was strongly inhibited and the fraction of active sites reached only 16% (entry 35). However, when $AlEt_3$ was added 10 s after the polymerization start (i.e. at ca. 25% monomer conversion), no significant change in the fraction of active sites was observed as compared to the 'alkyl-aluminum free' conditions (40%, entry 32). The authors then concluded that $AlEt_3$ affects only the formation of active sites in the initiation phase but not during the propagation steps. On

Accepted manuscript

another hand, when $AlMe_3$was added at the beginning of the polymerization, an induction period (ca. 40 s) was observed for the formation of active sites. The χ^* value finally reached 50% at longer reaction times (2 min), which is similar to experiments conducted without any CTA. However, if $AlMe_3$ was added after 10 s of polymerization, then the fraction of active sites dropped to 5% instead of 50% under the 'alkylaluminum-free' conditions. At longer polymerization time (2 min), the χ^* value only reached 30%, which is significantly below the 50–60% values obtained without any CTA. Hence, compared to $AlEt_3$, $AlMe_3$ is likely to affect both the initiation and the propagation phases. Noteworthy, when Al*i*Bu_3 was used under the same conditions, neither the polymerization nor the formation of active sites was altered [84].

5. Critical analysis of methods implemented and application studies

The large variety of techniques presented in this review translates the longstanding will of different research groups to establish a method, as generically applicable as possible, to quantify the fraction of active catalyst as well as to determine the different kinetic parameters related to a catalytic system. Despite all these efforts, the methods developed so far always bear some disadvantages that make them inappropriate for some polymerization conditions.

While kinetic modelling provides a more exhaustive set of data for catalytic systems (namely, the fraction of active sites χ^*, the rate constant of propagation, and sometimes those of initiation, termination and transfer) [34,35,37,39–44,46,48,50–57, 9], this approach seems to be the most demanding technique; it requires especially designed equipment (i.e. quench-flow apparatus), optimized operational protocols, and highly skilled manpower. In addition, the use of complex comprehensive kinetic models requires resolution of large systems of differential equations, whereas implementation of approximations or simplifications in those models may bring large uncertainties in the determination of rates; the relevance of the values thus determined may hence be questioned.

Accepted manuscript

The protocols of chemical labelling of precatalyst or of the propagating metal–polymeryl species (quench-labelling) offer an alternative way to access the concentration of active sites [C^*] in a more direct manner. They rely on the high inertness of the installed tagging group with respect to the active centers and on the high chemical selectivity of these reactions. However, both criterions are not always met. In the first case, the presence of the tagging group (e.g. an aromatic chromophore group [49]) in the close proximity to the active center may be detrimental to its regular performance, thus negatively influencing the kinetics of propagation. For the quench-labelling methods, the limited or sometimes poor selectivity of the reactions between the propagating metal–polymeryl species and the labeling reagent (CO [38,65,76–79], O_2 [85], Br_2 [87], TCC [91,92], etc) also results in errors in determination of active sites count. For example, all propagating species may not be systematically trapped by the quenching reagent, thus yielding underestimated sites counts. In contrast, in other cases, especially in alcoholysis protocols with MeO^2H [35,46,49–57,59] or MeO^3H [64–69], uncontrolled reactivity of the quench-labelling reagents with different types of metal–polymeryl species present in the polymerization mixture, notably those derived from transfer reactions (with Al, Zn, etc), can return significantly overestimated [C^*] values.

As evidenced from the investigations summarized in Part 4 of this review, a comprehensive critical analysis of the results presented here is largely hampered by the different conditions used. Also, as it is often difficult to apply strictly the same conditions with one technique of active sites count to another one, direct comparison of the same catalytic systems studied by different methods cannot be straightforwardly undertaken.

Nonetheless, several general comments can be made:

- In the cases where the quantity [C^*] could not be assessed via an independent method, the rate parameters were extracted with an activation efficiency value set arbitrarily (in most cases to 100%) [33,34]. The rate parameters thus determined are then obviously quite questionable.

Accepted manuscript

- Many models can efficiently reproduce only the initial part of the polymerization, when the molecular weight M_n grows linearly with time. Therefore, the values of activation efficiency and propagation rate constants are valid only for these early stages of the polymerization. Note, however, that this restriction is anyway valid for all systems, independently of the investigation method used, since intrinsic parameters (i.e., activation efficiency, speciation, etc) may well not remain constant over the polymerization course. As a consequence of a simplified model, the values returned may be less informative. For instance, the method used by Bochmann [39,40,44] and Busico [37,43] only returns an average value of k_p for active sites derived from both 1,2- and 2,1- olefin insertions. Also, these techniques are preferentially reserved for extremely productive catalyst systems that can generate over the time scale of the study a mass of polymer consequent enough for analysis.

- For a given catalyst system studied under the same or closely related conditions, but with different techniques, very different results in active sites count were reported. For example, Tait *et al.* claimed that 100% of Zr centers were active in the polymerization of ethylene with the Cp_2ZrCl_2/MAO system [78], but Chien *et al.* found only 10% of catalyst active [65]. Similar discrepancies were identified for other metallocene based systems (e.g. **5a** [58,92]). On the other hand, with the **5b**/$B(C_6F_5)_3$ system, very similar [C^*] values were obtained for polymerization of 1-hexene with different techniques [46,59,81]. This highlights the difficulties met in such studies, which depend not only on the efficiency of the counting and analytical techniques employed, but also of the sensitivity/complexity of the catalyst systems investigated.

6. Conclusions

The aim of this review is to highlight a common shortcoming often, not to say systematically, overlooked in modern homogeneous catalysis and, in particular, for Ziegler-Natta-type polymerization processes. While the activity of a catalytic system involved in a complex, multi-

Accepted manuscript

step process is mainly determined by the rate-determining step, that is in most cases d[substrate]/dt = –k[substrate][C^*], where [C^*] is the concentration of catalyst in its active form, it is generally assumed or accepted a quantitative transformation of the catalyst precursor into an active form (i.e., 100% activation efficiency); this is in particular applied for calculation of turnover number (TON) and turnover frequency (TOF) values.

As outlined in this review, it has been established by different, sometimes complementary, experimental techniques that for Ziegler-Natta-type polymerization processes, the typical concentration of active catalyst, [C^*], is often much inferior (<<50% of the concentration of precatalyst, $[C]_0$). Assessment of the fraction of active sites, $\chi^* = [C^*]/[C]_0$, is obviously a challenging task. An important issue that appears from this review is the identification of techniques, ready to implement, that selectively and quantitatively discern the catalytic sites effectively at work, leaving aside dormant sites and other metal species not directly involved in propagation. Hence, although significant progress has been achieved in recent years thanks to the awareness and ingeniousness of scientists regarding these issues, many χ^* values reported to date must still be considered with care, because of the intrinsic limitations of some methods. Yet, it appears clearly that the χ^* values depend very much on the nature of both precatalyst and cocatalyst/coactivator, as well as on experimental parameters, essentially intensive ones (temperature, solvent, etc).

The rational development of novel, more productive and selective polymerization catalytic systems requires a better understanding of their behavior. Therefore, a comprehensive kinetic analysis is required for an entire polymerization system (precatalyst + coactivator), to determine the rate constants relative to each step of the polymerization process: initiation, polymer chain growth (propagation) and termination/transfer. Besides, insight on possible deactivation processes resulting in decay of active sites is another mandatory information, which could be reasonably used for engineering more efficient catalytic systems reluctant towards side reactions.

Accepted manuscript

7. Acknowledgments

The authors thank Total Research and Technology Feluy and Total Corporate Research for continuous collaborative work. XD is grateful to Total Co. and ANRT for a PhD grant.

8. References

[1] A.L. McKnight, R.M. Waymouth, Group 4 ansa-Cyclopentadienyl-Amido Catalysts for Olefin Polymerization, Chem. Rev. 98 (1998) 2587–2598. doi:10.1021/cr940442r.
[2] H.G. Alt, A. Köppl, Effect of the Nature of Metallocene Complexes of Group IV Metals on Their Performance in Catalytic Ethylene and Propylene Polymerization, Chem. Rev. 100 (2000) 1205–1222. doi:10.1021/cr9804700.
[3] L. Resconi, L. Cavallo, A. Fait, F. Piemontesi, Selectivity in Propene Polymerization with Metallocene Catalysts, Chem. Rev. 100 (2000) 1253–1346. doi:10.1021/cr9804691.
[4] W. Kaminsky, The discovery of metallocene catalysts and their present state of the art, J. Polym. Sci. A Polym. Chem. 42 (2004) 3911–3921. doi:10.1002/pola.20292.
[5] W. Kaminsky, A. Laban, Metallocene catalysis, Appl. Catal., A. 222 (2001) 47–61. doi:10.1016/S0926-860X(01)00829-8.
[6] C. Janiak, F. Blank, Metallocene Catalysts for Olefin Oligomerization, Macromol. Symp. 236 (2006) 14–22. doi:10.1002/masy.200690047.
[7] V. Busico, Metal-catalysed olefin polymerisation into the new millennium: a perspective outlook, Dalton Trans. 0 (2009) 8794–8802. doi:10.1039/B911862B.
[8] H.H. Brintzinger, D. Fischer, Development of ansa-Metallocene Catalysts for Isotactic Olefin Polymerization, in: W. Kaminsky (Ed.), Polyolefins: 50 Years after Ziegler and Natta II, Springer Berlin Heidelberg, 2013: pp. 29–42. doi:10.1007/12_2013_215.
[9] M.C. Baier, M.A. Zuideveld, S. Mecking, Post-Metallocenes in the Industrial Production of Polyolefins, Angew. Chem. Int. Ed. 53 (2014) 9722–9744. doi:10.1002/anie.201400799.
[10] R.A. Collins, A.F. Russell, P. Mountford, Group 4 metal complexes for homogeneous olefin polymerisation: a short tutorial review, Appl. Petrochem. Res. 5 (2015) 153–171. doi:10.1007/s13203-015-0105-2.
[11] W. Kaminsky, M. Miri, H. Sinn, R. Woldt, Bis(cyclopentadienyl)zirkon-verbindungen und aluminoxan als Ziegler-Katalysatoren für die polymerisation und copolymerisation von olefinen, Makromol. Chem., Rapid Commun. 4 (1983) 417–421. doi:10.1002/marc.1983.030040612.
[12] J.A. Ewen, Mechanisms of stereochemical control in propylene polymerizations with soluble Group 4B metallocene/methylalumoxane catalysts, J. Am. Chem. Soc. 106 (1984) 6355–6364. doi:10.1021/ja00333a041.
[13] H. Sinn, W. Kaminsky, H.-J. Vollmer, R. Woldt, “Living Polymers” on Polymerization with Extremely Productive Ziegler Catalysts, Angew. Chem. Int. Ed. 19 (1980) 390–392. doi:10.1002/anie.198003901.
[14] F.R.W.P. Wild, M. Wasiucionek, G. Huttner, H.H. Brintzinger, ansa-Metallocene derivatives: VII. Synthesis and crystal structure of a chiral ansa-zirconocene derivative with ethylene-bridged tetrahydroindenyl ligands, J. Organomet. Chem. 288 (1985) 63–67. doi:10.1016/0022-328X(85)80104-2.
[15] W. Spaleck, F. Kueber, A. Winter, J. Rohrmann, B. Bachmann, M. Antberg, V. Dolle, E.F. Paulus, The Influence of Aromatic Substituents on the Polymerization Behavior of Bridged Zirconocene Catalysts, Organometallics. 13 (1994) 954–963. doi:10.1021/om00015a032.

Accepted manuscript

[16] W. Spaleck, M. Aulbach, B. Bachmann, F. Küber, A. Winter, Stereospecific metallocene catalysts: Scope and limits of rational catalyst design, Macromol. Symp. 89 (1995) 237–247. doi:10.1002/masy.19950890124.
[17] J.A. Ewen, R.L. Jones, A. Razavi, J.D. Ferrara, Syndiospecific propylene polymerizations with Group IVB metallocenes, J. Am. Chem. Soc. 110 (1988) 6255–6256. doi:10.1021/ja00226a056.
[18] A. Razavi, J.L. Atwood, Preparation and crystal structures of the complexes (η^5-C_5H_3Me-CMe_2-η^5-$C_{13}H_8$)MCl_2 (M = Zr or Hf): mechanistic aspects of the catalytic formation of a syndiotactic-isotactic stereoblock-type polypropylene, J. Organomet. Chem. 497 (1995) 105–111. doi:10.1016/0022-328X(95)00115-7.
[19] E. Kirillov, N. Marquet, A. Razavi, V. Belia, F. Hampel, T. Roisnel, J.A. Gladysz, J.-F. Carpentier, New C_1-Symmetric Ph_2C-Bridged Multisubstituted ansa-Zirconocenes for Highly Isospecific Propylene Polymerization: Synthetic Approach via Activated Fulvenes, Organometallics. 29 (2010) 5073–5082. doi:10.1021/om100289y.
[20] S.A. Miller, J.E. Bercaw, Mechanism of Isotactic Polypropylene Formation with C_1-Symmetric Metallocene Catalysts, Organometallics. 25 (2006) 3576–3592. doi:10.1021/om050841k.
[21] J. Okuda, Bifunctional Cyclopentadienyl Ligands in Organotransition Metal Chemistry, Comments Inorg. Chem. 16 (1994) 185–205. doi:10.1080/02603599408035859.
[22] P. Jutzi, U. Siemeling, Cyclopentadienyl compounds with nitrogen donors in the side-chain, J. Organomet. Chem. 500 (1995) 175–185. doi:10.1016/0022-328X(95)00514-Q.
[23] P.J. Shapiro, E. Bunel, W.P. Schaefer, J.E. Bercaw, Scandium complex [{(η^5-C_5Me_4)Me_2Si(η^1-$NCMe_3$)}(PMe_3)ScH]$_2$: a unique example of a single-component α-olefin polymerization catalyst, Organometallics. 9 (1990) 867–869. doi:10.1021/om00117a055.
[24] D.W. Carpenetti, L. Kloppenburg, J.T. Kupec, J.L. Petersen, Application of Amine Elimination for the Efficient Preparation of Electrophilic ansa-Monocyclopentadienyl Group 4 Complexes Containing an Appended Amido Functionality. Structural Characterization of [(C_5H_4)$SiMe_2$(N-t-Bu)]$ZrCl_2$(NMe_2H), Organometallics. 15 (1996) 1572–1581. doi:10.1021/om950858a.
[25] E.Y. Tshuva, I. Goldberg, M. Kol, Z. Goldschmidt, Zirconium Complexes of Amine−Bis(phenolate) Ligands as Catalysts for 1-Hexene Polymerization: Peripheral Structural Parameters Strongly Affect Reactivity, Organometallics. 20 (2001) 3017–3028. doi:10.1021/om0101285.
[26] E.Y. Tshuva, S. Groysman, I. Goldberg, M. Kol, Z. Goldschmidt, [ONXO]-Type Amine Bis(phenolate) Zirconium and Hafnium Complexes as Extremely Active 1-Hexene Polymerization Catalysts, Organometallics. 21 (2002) 662–670. doi:10.1021/om010493w.
[27] H. Makio, N. Kashiwa, T. Fujita, FI Catalysts: A New Family of High Performance Catalysts for Olefin Polymerization, Adv. Synth. Catal. 344 (2002) 477–493. doi:10.1002/1615-4169(200207)344:5<477::AID-ADSC477>3.0.CO;2-6.
[28] S. Matsui, M. Mitani, J. Saito, Y. Tohi, H. Makio, N. Matsukawa, Y. Takagi, K. Tsuru, M. Nitabaru, T. Nakano, H. Tanaka, N. Kashiwa, T. Fujita, A Family of Zirconium Complexes Having Two Phenoxy−Imine Chelate Ligands for Olefin Polymerization, J. Am. Chem. Soc. 123 (2001) 6847–6856. doi:10.1021/ja0032780.
[29] T. Matsugi, T. Fujita, High-performance olefin polymerization catalysts discovered on the basis of a new catalyst design concept, Chem. Soc. Rev. 37 (2008) 1264–1277. doi:10.1039/B708843B.
[30] T.R. Boussie, G.M. Diamond, C. Goh, K.A. Hall, A.M. LaPointe, M.K. Leclerc, V. Murphy, J.A.W. Shoemaker, H. Turner, R.K. Rosen, J.C. Stevens, F. Alfano, V. Busico, R. Cipullo, G. Talarico, Nonconventional Catalysts for Isotactic Propene Polymerization in Solution Developed by Using High-Throughput-Screening Technologies, Angew. Chem. Int. Ed. 45 (2006) 3278–3283. doi:10.1002/anie.200600240.

Accepted manuscript

[31] G.J. Domski, E.B. Lobkovsky, G.W. Coates, Polymerization of α-Olefins with Pyridylamidohafnium Catalysts: Living Behavior and Unexpected Isoselectivity from a C_s-Symmetric Catalyst Precursor, Macromolecules. 40 (2007) 3510–3513. doi:10.1021/ma062824s.
[32] S. Mehdiabadi, J.B.P. Soares, D. Bilbao, J. Brinen, Ethylene Polymerization and Ethylene/1-Octene Copolymerization with rac-Dimethylsilylbis(indenyl)hafnium Dimethyl Using Trioctyl Aluminum and Borate: A Polymerization Kinetics Investigation, Macromolecules. 46 (2013) 1312–1324. doi:10.1021/ma302513u.
[33] C.-H. Chen, W.-C. Shih, C. Hilty, In Situ Determination of Tacticity, Deactivation, and Kinetics in [*rac*-(C_2H_4(1-Indenyl)$_2$)ZrMe][$B(C_6F_5)_4$] and [Cp_2ZrMe][$B(C_6F_5)_4$]-Catalyzed Polymerization of 1-Hexene Using ^{13}C Hyperpolarized NMR, J. Am. Chem. Soc. 137 (2015) 6965–6971. doi:10.1021/jacs.5b04479.
[34] J.M.V. Estrada, A.E. Hamielec, Modelling of ethylene polymerization with Cp_2ZrCl_2/MAO catalyst, Polymer. 35 (1994) 808–818. doi:10.1016/0032-3861(94)90880-X.
[35] K.A. Novstrup, N.E. Travia, G.A. Medvedev, C. Stanciu, J.M. Switzer, K.T. Thomson, W.N. Delgass, M.M. Abu-Omar, J.M. Caruthers, Mechanistic Detail Revealed via Comprehensive Kinetic Modeling of [*rac*-C_2H_4(1-indenyl)$_2ZrMe_2$]-Catalyzed 1-Hexene Polymerization, J. Am. Chem. Soc. 132 (2010) 558–566. doi:10.1021/ja906332r.
[36] G. Natta, I. Pasquon, The Kinetics of the Stereospecific Polymerization of α-Olefins, in: P.W.S. and P.B.W. D.D. Eley (Ed.), Advances in Catalysis, Academic Press, 1959: pp. 1–66. doi:10.1016/S0360-0564(08)60416-2.
[37] V. Busico, R. Cipullo, V. Esposito, Stopped-flow polymerizations of ethene and propene in the presence of the catalyst system *rac*-Me_2Si(2-methyl-4-phenyl-1-indenyl)$_2ZrCl_2$/methylaluminoxane, Macromol. Rapid Commun. 20 (1999) 116–121. doi:10.1002/(SICI)1521-3927(19990301)20:3<116::AID-MARC116>3.0.CO;2-A.
[38] T. Shiono, M. Ohgizawa, K. Soga, Reaction of the Ti-polyethylene bond with carbon monoxide over the bis(cyclopentadienyl)titanium dichloride-methylaluminoxane catalyst system, Polymer. 35 (1994) 187–192. doi:10.1016/0032-3861(94)90070-1.
[39] F. Song, R.D. Cannon, M. Bochmann, Zirconocene-Catalyzed Propene Polymerization: A Quenched-Flow Kinetic Study, J. Am. Chem. Soc. 125 (2003) 7641–7653. doi:10.1021/ja029150v.
[40] F. Ghiotto, C. Pateraki, J.R. Severn, N. Friederichs, M. Bochmann, Rapid evaluation of catalysts and MAO activators by kinetics: what controls polymer molecular weight and activity in metallocene/MAO catalysts?, Dalton Trans. 42 (2013) 9040–9048. doi:10.1039/C3DT00107E.
[41] V.D. Schnell, G. Fink, Elementarprozesse der Ziegler-Natta-Katalyse. I. Oligomerenkinetik im Strömungsrohr, Angew. Makromol. Chem. 39 (1974) 131–147. doi:10.1002/apmc.1974.050390111.
[42] T. Keii, M. Terano, K. Kimura, K. Ishii, A kinetic argument for a quasi-living polymerization of propene with a $MgCl_2$-supported catalyst, Makromol. Chem. Rapid Commun. 8 (1987) 583–587. doi:10.1002/marc.1987.030081113.
[43] R. Cipullo, P. Melone, Y. Yu, D. Iannone, V. Busico, Olefin polymerisation catalysts: when perfection is not enough, Dalton Trans. 44 (2015) 12304–12311. doi:10.1039/C5DT01514F.
[44] F. Song, R.D. Cannon, S.J. Lancaster, M. Bochmann, Activator effects in metallocene-based alkene polymerisations: unexpectedly strong dependence of catalyst activity on trityl concentration, J. Mol. Catal. A: Chem. 218 (2004) 21–28. doi:10.1016/j.molcata.2004.03.042.
[45] M. Bochmann, S.J. Lancaster, M.D. Hannant, A. Rodriguez, M. Schormann, D.A. Walker, T.J. Woodman, Role of $B(C_6F_5)_3$ in catalyst activation, anion formation, and as C_6F_5 transfer agent, Pure Appl. Chem. 75 (2003) 1183–1195. doi:10.1351/pac200375091183.

Accepted manuscript

[46] Z. Liu, E. Somsook, C.B. White, K.A. Rosaaen, C.R. Landis, Kinetics of Initiation, Propagation, and Termination for the [*rac*-(C_2H_4(1-indenyl)$_2$)ZrMe][MeB(C_6F_5)$_3$]-Catalyzed Polymerization of 1-Hexene, J. Am. Chem. Soc. 123 (2001) 11193–11207. doi:10.1021/ja016072n.
[47] C.B. White, K.A. Rosaaen, C.R. Landis, A rapid quenched-flow device for the study of homogeneous polymerization kinetics, Rev. Sci. Instrum. 73 (2002) 411–415. doi:10.1063/1.1431441.
[48] M.M. Ranieri, J.-P. Broyer, F. Cutillo, T.F.L. McKenna, C. Boisson, Site count: is a high-pressure quenched-flow reactor suitable for kinetic studies of molecular catalysts in ethylene polymerization?, Dalton Trans. 42 (2013) 9049–9057. doi:10.1039/C3DT33004D.
[49] B.M. Moscato, B. Zhu, C.R. Landis, GPC and ESI-MS Analysis of Labeled Poly(1-Hexene): Rapid Determination of Initiated Site Counts during Catalytic Alkene Polymerization Reactions, J. Am. Chem. Soc. 132 (2010) 14352–14354. doi:10.1021/ja105775r.
[50] B.M. Moscato, B. Zhu, C.R. Landis, Mechanistic Investigations into the Behavior of a Labeled Zirconocene Polymerization Catalyst, Organometallics. 31 (2012) 2097–2107. doi:10.1021/om3000955.
[51] J.M. Switzer, N.E. Travia, D.K. Steelman, G.A. Medvedev, K.T. Thomson, W.N. Delgass, M.M. Abu-Omar, J.M. Caruthers, Kinetic Modeling of 1-Hexene Polymerization Catalyzed by Zr(tBu-ONNMe$_2$O)Bn$_2$/B(C_6F_5)$_3$, Macromolecules. 45 (2012) 4978–4988. doi:10.1021/ma300129n.
[52] D.K. Steelman, P.D. Pletcher, J.M. Switzer, S. Xiong, G.A. Medvedev, W.N. Delgass, J.M. Caruthers, M.M. Abu-Omar, Comparison of Selected Zirconium and Hafnium Amine Bis(phenolate) Catalysts for 1-Hexene Polymerization, Organometallics. 32 (2013) 4862–4867. doi:10.1021/om4006005.
[53] D.K. Steelman, S. Xiong, P.D. Pletcher, E. Smith, J.M. Switzer, G.A. Medvedev, W.N. Delgass, J.M. Caruthers, M.M. Abu-Omar, Effects of Pendant Ligand Binding Affinity on Chain Transfer for 1-Hexene Polymerization Catalyzed by Single-Site Zirconium Amine Bis-Phenolate Complexes, J. Am. Chem. Soc. 135 (2013) 6280–6288. doi:10.1021/ja401474v.
[54] D.K. Steelman, S. Xiong, G.A. Medvedev, W.N. Delgass, J.M. Caruthers, M.M. Abu-Omar, Effects of Electronic Perturbations on 1-Hexene Polymerization Catalyzed by Zirconium Amine Bisphenolate Complexes, ACS Catal. 4 (2014) 2186–2190. doi:10.1021/cs5003788.
[55] P.D. Pletcher, J.M. Switzer, D.K. Steelman, G.A. Medvedev, W.N. Delgass, J.M. Caruthers, M.M. Abu-Omar, Quantitative Comparative Kinetics of 1-Hexene Polymerization across Group IV Bis-Phenolate Catalysts, ACS Catal. 6 (2016) 5138–5145. doi:10.1021/acscatal.6b00974.
[56] A.Z. Preston, J. Kim, G.A. Medvedev, W.N. Delgass, J.M. Caruthers, M.M. Abu-Omar, Steric and Solvation Effects on Polymerization Kinetics, Dormancy, and Tacticity of Zr-Salan Catalysts, Organometallics. 36 (2017) 2237–2244. doi:10.1021/acs.organomet.7b00295.
[57] J.M. Switzer, P.D. Pletcher, D.K. Steelman, J. Kim, G.A. Medvedev, M.M. Abu-Omar, J.M. Caruthers, W.N. Delgass, Quantitative Modeling of the Temperature Dependence of the Kinetic Parameters for Zirconium Amine Bis(Phenolate) Catalysts for 1-Hexene Polymerization, ACS Catal. 8 (2018) 10407–10418. doi:10.1021/acscatal.8b01989.
[58] N. Naga, T. Shiono, T. Ikeda, Polymerization behavior of α-olefins with *rac*- and *meso*-type *ansa*-metallocene catalysts: Effects of cocatalyst and metallocene ligand, Macromol. Chem. Phys. 200 (1999) 1587–1594. doi:10.1002/(SICI)1521-3935(19990701)200:7<1587::AID-MACP1587>3.0.CO;2-5.

Accepted manuscript

[59] Z. Liu, E. Somsook, C.R. Landis, A ^{2}H-Labeling Scheme for Active-Site Counts in Metallocene-Catalyzed Alkene Polymerization, J. Am. Chem. Soc. 123 (2001) 2915–2916. doi:10.1021/ja0055918.
[60] J.C.W. Chien, C.-I. Kuo, Magnesium chloride supported high mileage catalyst for olefin polymerization. VII. Determinations of concentrations of titanium–polymer and aluminum–polymer bonds, J. Polym. Sci. Polym. Chem. 23 (1985) 731–760. doi:10.1002/pol.1985.170230310.
[61] J.C.W. Chien, C.-I. Kuo, Magnesium chloride supported high mileage catalyst for olefin polymerization. VIII. Decay and transformation of active sites, J. Polym. Sci. Polym. Chem. 23 (1985) 761–786. doi:10.1002/pol.1985.170230311.
[62] J.C.W. Chien, Y. Hu, Magnesium chloride supported high-mileage catalysts for olefin polymerization. XVII. Effect of lewis base on propylene polymerization, J. Polym. Sci. A Polym. Chem. 25 (1987) 2847–2870. doi:10.1002/pola.1987.080251020.
[63] J.C.W. Chien, Y. Hu, Magnesium chloride supported high-mileage catalysts for olefin polymerizations. XVIII. Effect of hydrogen and lewis bases, J. Polym. Sci. A Polym. Chem. 25 (1987) 2881–2892. doi:10.1002/pola.1987.080251022.
[64] J.C.W. Chien, B.-P. Wang, Metallocene–methylaluminoxane catalysts for olefin polymerization. I. Trimethylaluminum as coactivator, J. Polym. Sci. A Polym. Chem. 26 (1987) 3089–3102. doi:10.1002/pola.1988.080261117.
[65] J.C.W. Chien, B.-P. Wang, Metallocene–methylaluminoxane catalysts for olefin polymerizations. IV. Active site determinations and limitation of the ^{14}CO radiolabeling technique, J. Polym. Sci. A Polym. Chem. 27 (1989) 1539–1557. doi:10.1002/pola.1989.080270507.
[66] J.C.W. Chien, A. Razavi, Metallocene–methylaluminoxane catalyst for olefin polymerization. II. Bis-η^5-(neomenthyl cyclopentadienyl)zirconium dichloride, J. Polym. Sci. A Polym. Chem. 26 (1988) 2369–2380. doi:10.1002/pola.1988.080260910.
[67] J.C.W. Chien, R. Sugimoto, Kinetics and stereochemical control of propylene polymerization initiated by ethylene bis(4,5,6,7-tetrahydro-1-indenyl) zirconium dichloride/methyl aluminoxane catalyst, J. Polym. Sci. A Polym. Chem. 29 (1991) 459–470. doi:10.1002/pola.1991.080290402.
[68] J.C.W. Chien, W. Song, M.D. Rausch, Effect of counterion structure on zirconocenium catalysis of olefin polymerization, Macromolecules. 26 (1993) 3239–3240. doi:10.1021/ma00064a044.
[69] J.C.W. Chien, G.H. Llinas, M.D. Rausch, G.Y. Lin, H.H. Winter, J.L. Atwood, S.G. Bott, Two-state propagation mechanism for propylene polymerization catalyzed by *rac*-[anti-ethylidene(1-η^5-tetramethylcyclopentadienyl)(1-η^5-indenyl)] dimethyltitanium, J. Am. Chem. Soc. 113 (1991) 8569–8570. doi:10.1021/ja00022a080.
[70] V. Warzelhan, T.F. Burger, D.J. Stein, Über die bestimmung der zahl polymerisationsaktiver zentren von ziegler-natta-katalysatoren. Eine modifizierte methode mit ^{14}C-markierten kohlenstoffoxiden, Makromol. Chem. 183 (1982) 489–504. doi:10.1002/macp.1982.021830218.
[71] T. Shiono, M. Ohgizawa, K. Soga, Reaction between carbon monoxide and a Ti-polyethylene bond with a $MgCl_2$-supported $TiCl_4$ catalyst system, Makromol. Chem. 194 (1993) 2075–2085. doi:10.1002/macp.1993.021940720.
[72] J. Mejzlík, M. Lesná, Determination of active centers in heterogeneous Ziegler-Natta catalytic systems using carbon oxides, Makromol. Chem. 178 (1977) 261–266. doi:10.1002/macp.1977.021780127.
[73] J. Mejzlík, M. Lesná, J. Majer, Comparison of methods for determination of the number of active centers in Ziegler-Natta polymerizations, Makromol. Chem. 184 (1983) 1975–1985. doi:10.1002/macp.1983.021841003.
[74] G.D. Bukatov, V.S. Goncharov, V.A. Zakharov, Interaction of ^{14}CO with Ziegler-type heterogeneous catalysts and effect of interaction products on the determination of the

Accepted manuscript

amount of active centers, Makromol. Chem. 187 (1986) 1041–1051. doi:10.1002/macp.1986.021870501.
[75] M.M. Marques, P.J.T. Tait, J. Mejzlík, A.R. Dias, Polymerization of ethylene using high-activity Ziegler-type catalysts: Active center determination, J. Polym. Sci. A Polym. Chem. 36 (1998) 573–585. doi:10.1002/(SICI)1099-0518(199803)36:4<573::AID-POLA7>3.0.CO;2-Q.
[76] T.K. Han, Y.S. Ko, J.W. Park, S.I. Woo, Determination of the Number of Active Sites for Olefin Polymerization Catalyzed over Metallocene/MAO Using the CO Inhibition Method, Macromolecules. 29 (1996) 7305–7309. doi:10.1021/ma960023r.
[77] V. Busico, M. Guardasole, A. Margonelli, A.L. Segre, Insertion of Carbon Monoxide into Zr−Polymeryl Bonds: "Snapshots" of a Running Catalyst, J. Am. Chem. Soc. 122 (2000) 5226–5227. doi:10.1021/ja000657k.
[78] P.J.T. Tait, B.L. Booth, M.O. Jejelowo, The effect of ^{14}CO contact times on active centre determinations for the polymerization of ethylene catalysed by bis(η-cyclopentadienyl)zirconium(IV) dichloride/methylaluminoxane, Makromol. Chem., Rapid Commun. 9 (1988) 393–398. doi:10.1002/marc.1988.030090604.
[79] P.J.T. Tait, B.L. Booth, M.O. Jejelowo, Rate of Ethylene Polymerization with the Catalyst System (η^5-$RC_5H_4)_2ZrCl_2$—Methylaluminoxane, in: Catalysis in Polymer Synthesis, American Chemical Society, 1992: pp. 78–87. doi:10.1021/bk-1992-0496.ch006.
[80] J. Mejzlík, M. Lesná, J. Kratochvíla, Determination of the number of active centers in Ziegler-Natta polymerizations of olefins, in: Catalytical and Radical Polymerization, Springer Berlin Heidelberg, Berlin, Heidelberg, 1986: pp. 83–120. doi:10.1007/BFb0037613.
[81] D.L. Nelsen, B.J. Anding, J.L. Sawicki, M.D. Christianson, D.J. Arriola, C.R. Landis, Chromophore Quench-Labeling: An Approach to Quantifying Catalyst Speciation As Demonstrated for (EBI)$ZrMe_2$/$B(C_6F_5)_3$-Catalyzed Polymerization of 1-Hexene, ACS Catal. 6 (2016) 7398–7408. doi:10.1021/acscatal.6b01819.
[82] E.S. Cueny, H.C. Johnson, B.J. Anding, C.R. Landis, Mechanistic Studies of Hafnium-Pyridyl Amido-Catalyzed 1-Octene Polymerization and Chain Transfer Using Quench-Labeling Methods, J. Am. Chem. Soc. 139 (2017) 11903–11912. doi:10.1021/jacs.7b05729.
[83] H.C. Johnson, E.S. Cueny, C.R. Landis, Chain Transfer with Dialkyl Zinc During Hafnium–Pyridyl Amido-Catalyzed Polymerization of 1-Octene: Relative Rates, Reversibility, and Kinetic Models, ACS Catal. (2018) 4178–4188. doi:10.1021/acscatal.8b00524.
[84] E.S. Cueny, H.C. Johnson, C.R. Landis, Selective Quench-Labeling of the Hafnium-Pyridyl Amido-Catalyzed Polymerization of 1-Octene in the Presence of Trialkyl-Aluminum Chain-Transfer Reagents, ACS Catal. (2018) 11605–11614. doi:10.1021/acscatal.8b03615.
[85] R. Cipullo, S. Mellino, V. Busico, Identification and Count of the Active Sites in Olefin Polymerization Catalysis by Oxygen Quench, Macromolecular Chemistry and Physics. 215 (2014) 1728–1734. doi:10.1002/macp.201400156.
[86] G. Ciancaleoni, N. Fraldi, P.H.M. Budzelaar, V. Busico, R. Cipullo, A. Macchioni, Structure−Activity Relationship in Olefin Polymerization Catalysis: Is Entropy the Key?, J. Am. Chem. Soc. 132 (2010) 13651–13653. doi:10.1021/ja105965x.
[87] M. Vatamanu, B.N. Boden, M.C. Baird, An Investigation into the Identities and the Relative Concentrations of the Zr−Polymeryl Species Present during Ethylene and Propylene Polymerizations by Zirconocene-Based Ziegler Catalysts, Macromolecules. 38 (2005) 9944–9949. doi:10.1021/ma051947u.
[88] X. Shen, J. Hu, Z. Fu, J. Lou, Z. Fan, Counting the number of active centers in $MgCl_2$-supported Ziegler–Natta catalysts by quenching with 2-thiophenecarbonyl chloride and study on the initial kinetics of propylene polymerization, Catal Commun. 30 (2013) 66–69. doi:10.1016/j.catcom.2012.11.001.

Accepted Manuscript

[89] J. Hu, B. Han, X. Shen, Z. Fu, Z. Fan, Probing the roles of diethylaluminum chloride in propylene polymerization with $MgCl_2$-supported ziegler-natta catalysts, Chin. J. Polym. Sci. 31 (2013) 583–590. doi:10.1007/s10118-013-1260-5.
[90] X. Shen, Z. Fu, J. Hu, Q. Wang, Z. Fan, Mechanism of Propylene Polymerization with $MgCl_2$-Supported Ziegler–Natta Catalysts Based on Counting of Active Centers: The Role of External Electron Donor, J. Phys. Chem. C. 117 (2013) 15174–15182. doi:10.1021/jp404416n.
[91] Y. Guo, F. He, Z. Zhang, A. Khan, Z. Fu, J. Xu, Z. Fan, Influence of trimethylaluminum on kinetics of *rac*-Et$(Ind)_2ZrCl_2$/aluminoxane catalyzed ethylene polymerization, J. Organomet. Chem. 808 (2016) 109–116. doi:10.1016/j.jorganchem.2016.02.024.
[92] Y. Guo, Z. Zhang, W. Guo, A. Khan, Z. Fu, J. Xu, Z. Fan, Kinetics and mechanism of metallocene-catalyzed olefin polymerization: Comparison of ethylene, propylene homopolymerizations, and their copolymerization, J. Polym. Sci. A Polym. Chem. 55 (2017) 867–875. doi:10.1002/pola.28439.
[93] G. Fink, D. Schnell, Elementarprozesse der Ziegler-Katalyse. IV. Kinetische Auswertung der im Strömungsrohr erzeugten Oligomerenverteilungen, Angew. Chem. Int. Ed. 105 (1982) 39–48. doi:10.1002/apmc.1982.051050105.
[94] G. Ciancaleoni, N. Fraldi, P.H.M. Budzelaar, V. Busico, A. Macchioni, Activation of a bis(phenoxy-amine) precatalyst for olefin polymerisation: first evidence for an outer sphere ion pair with the methylborate counterion, Dalton Trans. 0 (2009) 8824–8827. doi:10.1039/B908805A.

Accepted manuscript